MODELING AND SIMULATION OF NEUROCYCLE ENZYME SYSTEM: BIFURCATION ANALYSIS

A PROJECT REPORT

Submitted in partial fulfillment for the award of the degree of

B.Tech

in

CHEMICAL ENGINEERING

by

KRITIKA KASHYAP

13BCH0011

School of Civil and Chemical Engineering

MAY & 2017

DECLARATION BY THE CANDIDATE

I here by declare that the project report entitled "**MODELING AND SIMULATION OF NEUROCYCLE ENZYME SYSTEM : BIFURCATION ANALYSIS"** submitted by me to Vellore Institute of Technology University, Vellore in partial fulfillment of the requirement for the award of the degree of **B.Tech** in **Chemical Engineering** is a record of bonafide project work carried out by me under the guidance of **PROFESSOR ANAND VEERABADRA PRASAD GURUMOORTHY**. I further declare that the work reported in this project has not been submitted and will not be submitted, either in part or in full, for the award of any other degree or diploma in this institute or any other institute or university.

Place : Vellore Signature of the Candidate

Date:

School of Civil and Chemical Engineering

CERTIFICATE

This is to certify that the project report entitled "**MODELING AND SIMULATION OF NEUROCYCLE ENZYME SYSTEM : BIFURCATION ANALYSIS"** submitted by **KRITIKA KASHYAP(13BCH0011)** to Vellore Institute of Technology University, Vellore, in partial fulfillment of the requirement for the award of the degree of B.Tech in chemical engineering is a record of bona fide work carried out by her under my guidance. The project fulfills the requirements as per the regulations of this Institute and in my opinion meets the necessary standards for submission. The contents of this report have not been submitted and will not be submitted either in part or in full, for the award of any other degree or diploma and the same is certified.

Guide HOD

Internal Examiner External Examiner

ACKNOWLEDGEMENT

I would like to extend my thanks and appreciation to my supervisor **Professor ANAND VEERABADRA PRASAD GURUMOORTHY** for helping me during the course of this project. He provided a motivating, enthusiastic, and critical atmosphere during the discussions we had. It is a great pleasure for me to conduct this project under his supervision. His valuable advice, guidance and encouragement led to the successful completion of the project. I am also thankful to the staff members of the Chemical Engineering Department, VIT University, Vellore for their assistance throughout the project work.

Place : Vellore

(KRITIKA KASHYAP)

Date :

TABLE OF CONTENTS

ABSTRACT

Chaos and Bifurcation are very important phenomena affecting many chemical and physical systems. They are related to the stability/instability and multiplicity phenomena associated with these systems. The neurocycle of the acetylcholine (ACh) transmitter in the brain exhibits the bifurcation phenomena and chaotic behavior. The effects of hydrogen ion feed concentrations, acetylcholinesterase (AChE) and β-amyloid aggregates on the activity of acetylcholine neurocycle have been investigated via the two-enzyme/two-compartment (2E2C) model where the presynaptic neuron is considered as compartment 1 while both the synaptic cleft and postsynaptic neuron are considered as compartment 2. Detailed analysis over a wide range of parameters is carried out to uncover dynamic solutions for concentrations of generated β-amyloid, ACh, choline, acetate and pH in compartments 1 and 2. Some of the obtained results relate to the phenomena occurring in the physiological experiments like periodic stimulation of neural cells and irregular functioning of acetylcholine receptors. The model depends on real kinetic expressions and parameters obtained from the literature, so the results can be used to direct a systematic research on cholinergic disorders like Alzheimer's Disease (AD) and Parkinson's Disease (PD) which are associated with the poor performance of the neurotransmitter acetylcholine.

NOTATIONS

$[H^+]$ hydrogen ions concentration (kmol/m^3)

$[OH^-]$ hydroxyle ions concentration (kmol/m^3)

$[S_1]$ acetylcholine concentration (kmol/m^3) (ACh)

$[S_2]$ choline concentration (kmol/m^3) (Ch)

$[S_3]$ acetyl CoA concentration (kmol/m^3)

AB β-amyloid concentrations

$[S_N]$ substrate N (catalyzed by enzyme N)

[a] acetate concentration (kmol/m^3)

[AC] Acetic acid concentration (kmol/m^3)

$\overline{\text{AChE}}$ concentration of acetylcholinesterase enzyme in compartment 2 (kg $\overline{\text{enzyme}}/m^3$)

CoA concentration of coenzyme A in compartment 1 (kg enzyme/m^3)

$\overline{\text{ChAT}}$ concentration of cholineacetyltransferase in compartment 1 (kg enzyme/m^3)

$\overline{\text{ACoA synthase}}$ concentration of Acetyl CoA Synthase in compartment 1 (kg enzyme/m^3)

K_{s1}, K_{h1} kinetic constants for the cholineacetyltransferase catalyzed reaction (kmol/m^3)

K_{s2}, K_h kinetic constants for the coenzyme A catalyzed reaction (kmol/m^3)

K_{s3}, K_{i3}, K_{hh3} kinetic constants for the acetylcholinesterase catalyzed reaction (kmol/m^3)

K_{bA1} kinetic constants for β-amyloid aggregates (kmol/m^3)

K_{L2} β-amyloid input rates

K_{L3}, K_{L4} kinetic constants for β-amyloid aggregates

K_W equilibrium constant for water (kmol^2/m^6)

α'_{H^+} membrane permeability for hydrogen ions (m/s)

α'_{OH^-} membrane permeability for hydroxyl ions (m/s)

α'_{S1} membrane permeability for acetylcholine (m/s)

α'_{S2} membrane permeability for choline (m/s)

α'_{S3} membrane permeability for acetyl CoA (m/s)

α'_{A} membrane permeability for acetate (m/s)

α'_{AC} membrane permeability for acetic acid (m/s)

A_M area of membrane separating compartments 1 and 2 (m^2)

q volumetric flow rate (m^3/s)

$R_{W(j)}$ rate of water formation in compartment j (kmol/m^3s)

$R_{(j)}$ rate of reaction in compartment j (kmol/m^3s)

R	recycle flow rate ratio
$V_{(j)}$	volume of compartment j (m^3)
E_N	enzyme N
P_N	reaction product N (produced by S_N catalyzed by (E_N)
V_R	V_1/V_2

LIST OF ABBREVIATIONS

AChE	Acetylcholinesterase
ChAT	Cholineacetyltranseferase
CoA	Coenzyme A
ACh	Acetylcholine
CSTR	Continuous Stirred Tank Reactor

SUBSCRIPTS

1	Compartment 1
2	Compartment 2
f	Feed condition

DIMENSIONLESS PARAMETERS

$h_j = [H^+]_j/K_{h1}$	hydrogen ion concentration
$s_{1j} = [S_1]_j/K_{S1}$	acetylcholine concentration
$s_{2j} = [S_2]_j/[S_2]_{ref}$	choline concentration
$s_{3j} = [S_3]_j/[S_3]_{ref}$	acetate concentration
$T = q.t/V_t$	time
$\gamma = K_w/ K_{i1}$	kinetic parameter
$\delta = K_{h1}/ K_{hh1}$	kinetic parameter
$\alpha = K_{s1}/ K_{i1}$	kinetic parameter
$\alpha_{H^+} = \alpha'_{H^+}. A_M/q$	membrane permeability (H^+)
$\alpha_{OH^-} = \alpha'_{OH^-}. A_M/q$	membrane permeability(OH^-)
$\alpha_{S1} = \alpha'_{S1}. A_M/q$	membrane permeability(S_1)
$\alpha_{S2} = \alpha'_{S2}. A_M/q$	membrane permeability(S_2)
$\alpha_{S3} = \alpha'_{S3}. A_M/q$	membrane permeability(S_3)

LIST OF FIGURES

LIST OF TABLES

1. INTRODUCTION

1.1 BACKGROUND

Acetylcholine (ACh) plays a central role in fundamental processes such as learning, memory, sleep and muscle contraction in mammals. Understanding of the mechanisms for ACh regulation would provide fundamental knowledge on the regulatory characteristics of the transmitter in the molecular processes of the chemical transmission. The regulatory mechanisms are based on regulation of the enzymatic reactions for synthesis and degradation of transmitters. The ACh neurocycle implies a coupled twoenzymes/two-compartments model with two strongly coupled events as follows:

The activation event: Acetylcholine is synthesized from choline and acetyl coenzyme A (Acetyl-CoA) by the enzyme choline acetyltransferase (ChAT) and is immediately stored in small vesicular compartments closely attached to the cytoplasmic side of the presynaptic membranes.

R_1 :

$$\text{Choline} + \text{Acetyl-CoA} \longrightarrow \text{Acetylcholine} + \text{CoA}$$

The degradation event: Once acetylcholine has completed its activation duty, the synaptic cleft degradation begins to remove the remaining acetylcholine. This occurs through the destruction of acetylcholine by hydrolysis that uses the acetylcholinesterase enzyme (AchE) to form choline and acetic acid.

R_2 :

$$\text{Acetylcholine} + H_2O \longrightarrow \text{Choline} + \text{Acetate} + H^+$$

The ACh neurocycle system consists of two compartments separated by a permeable membrane. The presynaptic neuron ending is the first compartment in which the biosynthesis reaction of ACh occurs catalyzed by the enzyme of cholineacetyltransferase (ChAT) by the acetyl-CoA and choline substrates. In the synaptic cleft as the other compartment, the ACh molecules are released from the first compartment to interact with the ACh receptor causing the signal transmission and a fast hydrolysis reaction into choline and acetate occurs and is catalyzed by the enzyme of acetylcholinesterase (AChE). Each compartment is open with relevant influxes and effluxes. The reaction products are reused in other metabolic reactions where CoA is utilized for production of Acetyl-CoA and choline is re-uptaken from the synaptic cleft to the presynaptic neuron for re-synthesis of ACh.

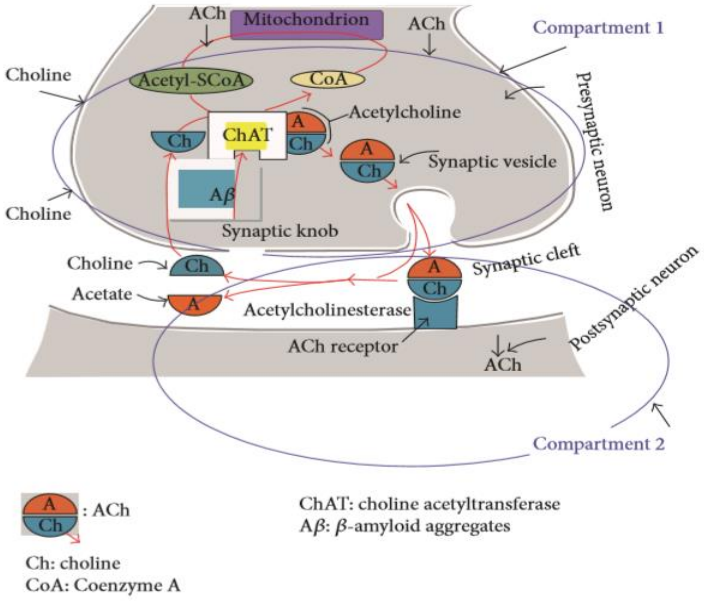

Figure 1.1: Schematic representation of ACh neurocycle

Since the behavior of neurotransmitter mechanisms represents a great challenge for understanding cholinergic diseases such as Alzheimer's and Parkinson's diseases, it is very important to understand the cholinergic system behavior. For my project, mathematical tools such as bifurcation analysis, well established nonlinear dynamics, and computer simulation are applied for modeling and prediction of complex behavior of the ACh neurocycle behavior. The method of bifurcation analysis and computer simulation are now established as an effective procedure for dynamic analysis and have been applied to obtain much knowledge of the dynamic behavior of metabolic pathways. Based on the regulating kinetic mechanisms of the enzymatic reactions, mathematical models can be established, and then the entire time course under different initial conditions and system environments and various flow rates of metabolites can be employed in terms of the change of system parameters by numerically integrating the rate equations.
Bifurcation theory is a mathematical discipline that deals with nonlinear phenomena. It investigates the stability and dynamics in non-linear systems. In bifurcation investigation a branch of solutions can be obtained by varying one parameter of the system and then the stability of the solution changes can be obtained. In the ACh cholinergic systems, numerical bifurcation analysis is well established with MATLAB software.

According to Chaos theory, chaos can be defined as the disorder of a system where it opposes relevant rules; this definition is consistent with the concept of instability of dynamical systems discovered primarily by the French physicist: Henri Poincare in the early 20th century. Chaos theory points to an apparent unpredictability. Chaos theory started with some of ideas related to irregularities in the universe such as arrhythmic beats of a human heart and fluid turbulence, then it has developed with wide ideas and can be described by the term complexity.

1.2. RESEARCH OBJECTIVE

1) Investigating the bifurcation behavior using feed parameters such as feed ACh, feed choline, feed acetyl Co-A in addition to feed hydrogen ions and AChE activity enzymes as bifurcation parameters and performing dynamics simulations at different parameter values and obtaining dynamic characteristics by monitoring the periodic and chaotic behaviors and studying the interaction between these findings and Alzheimer's and Parkinson's diseases.
2) The brain of Alzheimer's disease (AD) is characterized by accumulations of β-amyloid peptide aggregates which promote neurodegenerative dysfunction. Comprehensive understanding of the interaction between β-amyloid aggregates and acetylcholine (ACh) neurocycle will uncover the physiological processes related to AD and might result in improving therapeutic approaches for AD.
3) Studying the dynamic behavior and investigating the parameters and initial conditions values which achieve periodic and chaotic behaviours in addition to estimating the routes to fully developed chaos.
4) Estimating the most important factors in the ACh processes from the parametric study.

1.3. SCOPE OF THE PROJECT

This project focuses on discovering the dynamic behavior and the regulatory mechanism in Acetylcholine neurocycle system and the functioning of chemical transmission. Some kinetic regulatory mechanisms and dynamic aspects in the ACh neurocycle at the synapse are studied. In this project a mathematical model is used to represent the fundamental processes in the chemical transmission and dynamic analysis bifurcation and computer simulation are performed to reveal the dynamic aspects of regulation of ACh level in the presynaptic and postsynaptic terminals for signal transmission and the regulatory function of AChE enzymes. The scope of the project is as follows:

1) Understanding the kinetic mechanisms for enzymatic processes which are hydrogen proton (which is relevant to pH) dependent and substrates dependent: The first mechanism is for synthesis of ACh in the presynaptic terminal from choline and acetyl Co-A catalyzed by the enzyme ChAT and the other is for hydrolysis of ACh in the postsynaptic cleft into choline and acetate by the enzyme AChE. These mechanisms are based on the nature of interactions between both compartments and lead to deriving reasonable rate equations and describe synthesis and hydrolysis reactions accurately. The synthesis and hydrolysis of ACh are analyzed on the level of single vesicles, rather than at that of the whole nervous system.
2) The dynamic process models are used to simulate the complete neurocycle of the ACh as a simplified feedback two enzyme/two-compartment system. Each compartment is described as a constant flow, constant volume, isothermal, continuous stirred tank reactor (CSTR). The presynaptic and postsynaptic cells are represented by these two compartments separated by a permeable membrane assuming that all the events are homogeneous in all vesicles, and using the proper dimensionless state variables and parameters. Using dynamic mole balances for the chemical species involved in the enzymatic neurocycle of the neurotransmitter a set of differential equations have been derived which accurately describe the system. Nonlinearity of this set of highly non-linear balance equations gives us preliminary insight into the bifurcation and chaotic behavior of this complex biological system.
3) The dynamic behavior of the interaction between β-amyloid peptide aggregates and cholinergic neurocycle are studied. This can occur when β-amyloid peptide aggregates interact with the enzyme ChAT which is responsible for the synthesis of ACh in compartment 1. Three different kinetic mechanisms account for the interaction between β-amyloid aggregates and ChAT activity. In the first and second kinetic mechanisms, β-amyloid aggregate is supposed to attack different species in the enzyme. In the third kinetic mechanism, all species in ChAT are attacked by β-amyloid aggregates.
4) The bifurcation behaviour is studied using the feed parameters and enzyme activities as bifurcation parameters and dynamics simulations are carried out for different parameter values. Therefore, many dynamic characteristics are obtained by studying monitoring the periodic and chaotic behaviors.

2. PROJECT DESCRIPTION

Acetylcholine (ACh) serves as the transmitter of nerve impulses at cholinergic synapses. ACh plays a vital role in the memory excitations and such vital functions such as learning, thinking, sleep and cognition. It is released from the presynaptic neurons in various concentrations. After ACh is released from the presynaptic neuron, it is received by ACh cholinergic receptors (AChr), located in the postsynaptic membrane, to induce chemical and electrical signals. There are two substrates required for the biosynthesis of ACh: choline and acetyl coenzyme A (acetyl-CoA). There are two enzymes: the first one is the enzyme choline acetyltransferase (ChAT) which catalyzes the biosynthesis of ACh in the presynaptic neurons; the other is the enzyme acetylcholinesterase (AChE) which catalyzes the hydrolysis of ACh in the synaptic cleft. It is clear that the presynaptic neurons require three substances: ChAT, acetyl-CoA and choline. Acetyl-CoA is the only substance which is synthesized directly in the presynaptic terminals. However, choline is the only product which is synthesized outside of the presynaptic neurons. It is supplied from the extracellular fluid and degradation of ACh.

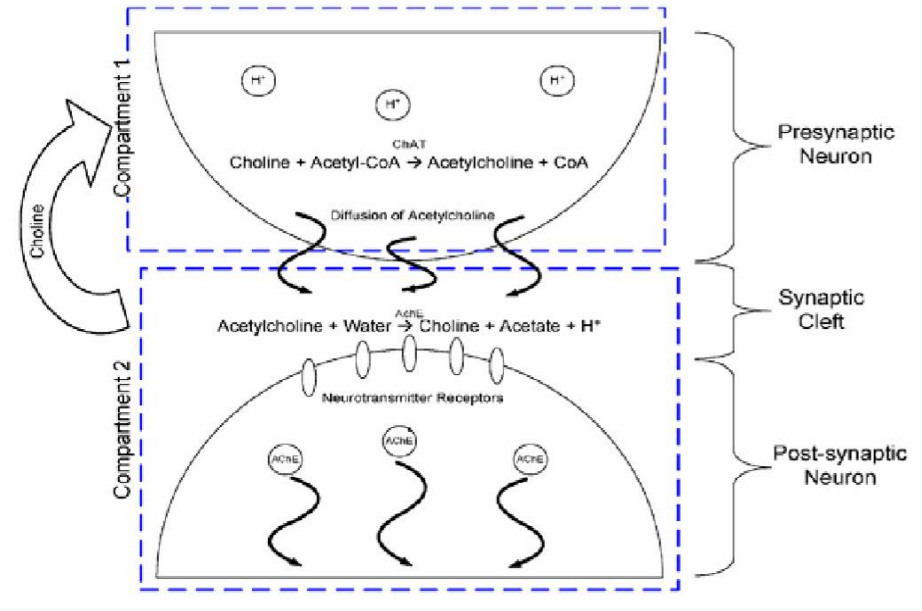

Figure 2.1: Schematic of synaptic neurons and cleft

As shown in Figure 2.1, a complete neurocycle of ACh constitutes a coupled two-enzyme system with the following two simultaneous events: Firstly, in the presynaptic neuron, ChAT

catalyzes the synthesis reaction from choline and acetyl CoA substrates, then ACh is stored in the vesicles which transport through the cytoplasm of the neuron to be fused with the presynaptic membranes to give the opportunity for ACh release in the synaptic cleft. Secondly, as soon as ACh has been received by the postsynaptic receptors and finished its excitation job, the hydrolysis reactions catalyzed by the acetyl cholinesterase (AChE) to form choline and acetic acid starts. Because choline cannot be synthesized inside brain, brain depends on other resources for getting choline. There are two sources for choline in the fluid existing in the environment outside neurons inside the brain: the first one is the free choline of the blood plasma and the second one is the brain cells, where it has been released from choline containing compounds. Choline produced in synaptic gaps by the hydrolysis of ACh is re-utilized for the synthesis of ACh in presynaptic nerve endings. Therefore, choline recycled plays an important role in the synthesis of ACh. Because hydrogen protons are released in the enzymatic reactions, the pH is declined. Furthermore, the appeared hysteresis behavior is developed for a certain range of parameters due to the hydrogen protons production which will cause itself an auto- catalytic influence in addition to the presence of diffusion effects. For this project two kinetic mechanisms are studied: one is for the synthesis of ACh by the enzyme ChAT and the other is for the hydrolysis of ACh by the enzyme AChE. The mathematical expressions for both reactions are derived to obtain reasonable rate equations. These models try to analyze the synthesis and hydrolysis of ACh at the level of a single vesicle, rather than the whole nervous system. In this chapter diffusion-reaction models are presented. Real kinetic mechanisms are used to get more reasonable and precise kinetic synthesis and hydrolysis rate equations by considering realistic kinetic schemes. The model is built based on new considerations such as ChAT synthesis and AChE hydrolysis reactions in the first compartment and other physiological considerations such as the recycle effects of choline from the synaptic cleft to the presynaptic neurons. The numerical task is to solve the Initial Value Problem given by the eight differential equations in Table 3.1 with the given 26 system parameters and the two rate equations for any physically feasible set of initial values $\Psi(0)$ and feed parameters Ψfeed numerically. A numerical solution of the problem may consist of a plot of all eight profiles $h_1(t)$, $s_{11}(t)$, $s_{21}(t)$, $s_{31}(t)$, $h_2(t)$, $s_{12}(t)$, $s_{22}(t)$, and $s_{33}(t)$ for a certain time interval $0 \leq t \leq$ Tend. Or it may involve phase plots, such as that of the acetylcholine concentration in compartment (1) versus that in compartment (2). The aim in the computations that follow is to show the variations in the quality of the solutions for differing values of hf (the hydrogen ion concentration of the feed), acetylcholinesterase (AChE) and β-amyloid aggregates to compartment (1).

3. TECHNICAL SPECIFICATION AND DESIGN APPROACH

3.1 THE TWO-ENZYME /TWO COMPARTMENT MODEL

Figure 2.2 demonstrates the two compartments of ChAT/AChE system. The first compartment represents the presynaptic terminal, and the second compartment represents the synaptic cleft and the postsynaptic neuron. Every compartment is assumed to be a continuous stirred tank reactor (CSTR), isothermal, constant volume, constant flow, and the two compartments are divided by a permeable membrane. The ionization of the acetic acid is assumed to be completely in order to simplify the solution of the model. All events and reactions are supposed to be in homogenous systems. All state variables and parameters are described in the dimensionless form.

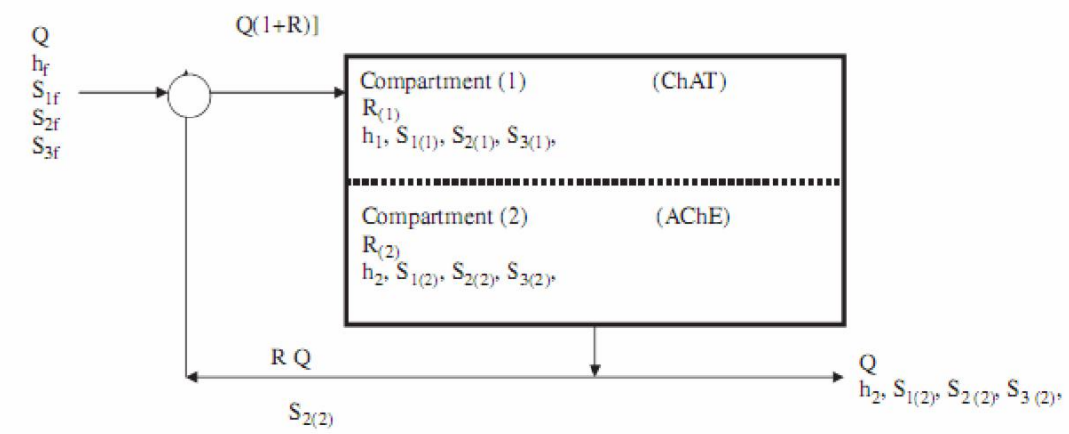

Figure 3.1: Two enzyme/two compartment model

3.2 MODEL ASSUMPTIONS: EFFECTS OF h_f AND $\overline{\text{AChE}}$

1) Compartment 1 represents the presynaptic terminal neuron where ACh is synthesized from choline and acetyl CoA as substrates and catalyzed by the enzyme ChAT. However, compartment 2 consists of two main parts: the postsynaptic neuron and the synaptic cleft where both parts are lumped together into one homogeneous compartment representing a unified compartment which is compartment 2 instead of 3 or 4 or 5 compartments because both the synaptic cleft and the postsynaptic neurons are harmonized and interactive. This in

addition for the purpose of avoiding the expected complexity and difficulty in solving the model and analyzing the results when the dimensionality is too high.

2) The concentrations of substances in compartment 2 represent the average concentrations in both the synaptic cleft and the post-synaptic neuron.

3) Each compartment is assumed to be homogenous; this means we neglect the internal mass transfer limitations between the cytoplasm and the synaptic vesicles in compartment 1 and the diffusion between ACh and the postsynaptic receptors in compartment 2.

4) Both compartments are assumed to be separated by a completely permeable membrane.

5) No product inhibition in both compartments. However, the synthesis reaction catalyzed by the enzyme ChAT in compartment 1 is assumed to be inhibited by the choline substrate as the limiting substrate and acetyl CoA. In addition, compartment 2 is assumed to be inhibited by ACh as the substrate.

6) The transport of substances from compartment 1 to compartment 2 is via passive diffusion, however, the transport of choline from compartment 2 to compartment 1 is via facilitated diffusion.

7) Changes in hydrogen proton concentrations in compartments 1 and 2 causing an autocatalytic effect between compartments 1 and 2 and is represented with a concentration gradient as the driving force for the transport from compartment 1 to compartment 2. The effects of potential differences occurred because of the unequal distribution of salts such as Na, K and Cl are ignored.

8) The system is isothermal, thus no effect with variation of temperature.

9) The dissociation of acetic acid is ignored in chapters 3, 4, and 5, and is taken into consideration at equilibrium as shown in chapter 5.

10) Both volumes of compartment 1 and 2 are assumed to be constant and equal V_1 and V_2 respectively.

11) Because compartment 1 includes the size of the presynaptic terminal and compartment 2 represents both the synaptic cleft and the surface of the postsynaptic neurons. Thus, compartment 1 is assumed to be larger than compartment 2 with the ratio $V_R=V_1/V_2$.

12) The recycle ratio is taken from Tucek et al (1990, 1985 and 1978); where choline produced from the hydrolysis of ACh in compartment 2 supplies choline with a high percent around 40-80% of the required choline for the synthesis reactions catalyzed by ChAT in compartment 1. 13) Each of the feed stream of axonal feed ACh (S_{1f}), the feed stream of plasma choline and choline produced from the release of phospholipids (S_{2f}), the feed stream of acetyl CoA coming from mitochondria (S_{3f}), and the feed stream of hydrogen protons

coming from the metabolic reactions and ionization of water (h_f), are collected together in a constant flow rate (q) to meet the choline recycle stream before entering the presynaptic neuron.

14) Both the feed flow rate to compartment 1 and the exit flow rate from compartment 2 are assumed to be constant at q (m^3/sec).

15) The diffusion and reaction events occurring in both contacted cholinergic neurons are explained by the two-enzyme two-compartment model.

All state variables, parameters, and rate equations are in the dimensionless form as given in Table 3.1. The system is 8 dimensions, where there are non-linear eight ordinary differential equations.

Table 3.1: Dimensionless forms of ordinary differential equations of 8 state variables

Item	Compartment	Differential equation
Hydrogen protons	1	$\frac{dh_{(1)}}{dT} = h_f - \gamma_1\left(\frac{1}{h_f}\right) - \alpha_H(h_{(1)} - h_{(2)}) + \alpha_{OH}\gamma_1\left(\frac{1}{h_{(1)}} - \frac{1}{h_{(2)}}\right)$
	2	$\frac{dh_{(2)}}{dT} = V_R\left(\alpha_H(h_{(1)} - h_{(2)}) - \alpha_{OH}\gamma_1\left(\frac{1}{h_{(1)}} - \frac{1}{h_{(2)}}\right) - \left(h_{(2)} - \frac{\gamma_1}{h_{(2)}}\right) + \frac{B_2}{k_{h1}}r(2)\right)$
Acetylcholine	1	$\frac{ds_{1(1)}}{dT} = s_{1f} - \alpha_{S_1}(s_{1(1)} - s_{1(2)}) + \frac{B_1 r(1)}{K_{s_1}}$
	2	$\frac{ds_{1(2)}}{dT} = V_R\left(\alpha_{S_1}(s_{1(1)} - s_{1(2)}) - s_{1(2)} - \frac{B_2 r(2)}{K_{s_1}}\right)$
Choline	1	$\frac{ds_{2(1)}}{dT} = s_{2f} + R^* s_{2(2)} - \alpha_{S_2}(s_{2(1)} - s_{2(2)}) - \frac{B_1}{S_{2\ refernce}}r(1)$
	2	$\frac{ds_{2(2)}}{dT} = V_R\left(\alpha_{S_2}(s_{2(1)} - s_{2(2)}) - (1+R)^* s_{2(2)} + \frac{B_2}{S_{2\ reference}}r(2)\right)$
Acetate	1	$\frac{ds_{3(1)}}{dT} = s_{3f} - \alpha_{S_3}(s_{3(1)} - s_{3(2)}) - \frac{B_1}{S_{3\ refernce}}r(1)$
	2	$\frac{ds_{3(2)}}{dT} = V_R\left(\alpha_{S_3}(s_{3(1)} - s_{3(2)}) - s_{3(2)} + \frac{B_2}{S_{3\ refernce}}r(2)\right)$
Rate of synthesis (r_1)	1	$r_{(1)} = \frac{\theta_1 s_{2(1)} s_{3(1)}}{\theta_2/h_{(1)}(h_{(1)} + 1 + \delta h_{(1)}^2) + \theta_3 s_{3(1)} + \theta_4 s_{2[1]} + \theta_5 s_{2(1)} s_{3(1)}}$
Rate of hydrolysis (r_2)	2	$r_{(2)} = \frac{s_{1(2)}}{s_{1(2)} + 1/h_{(2)}(h_{(2)} + 1 + \delta h_{(2)}^2) + \alpha s_{1(2)}^2}$

3.3 PROPOSED MECHANISMS FOR ENZYMATIC PROCESSES OF ACh

3.3.1 MECHANISM OF HYDROLYSIS OF ACh IN COMPARTMENT 2

The full mechanism for the pH dependent AChE kinetics is shown in Figure 3.2. The vertical direction represents the main reaction path. The active enzyme species presents in equilibrium with inactive protonated and de-protonated forms. The pH controls the system. E_1 is the active form of the enzyme; E_1H^* and E_1- are the protonated and de-protonated inactive enzyme forms. E_1S_1 and E_1^* are enzyme intermediate complexes. The substrate can combine with E_1S_1 to form another complex E_1^* that cannot react further to give product.

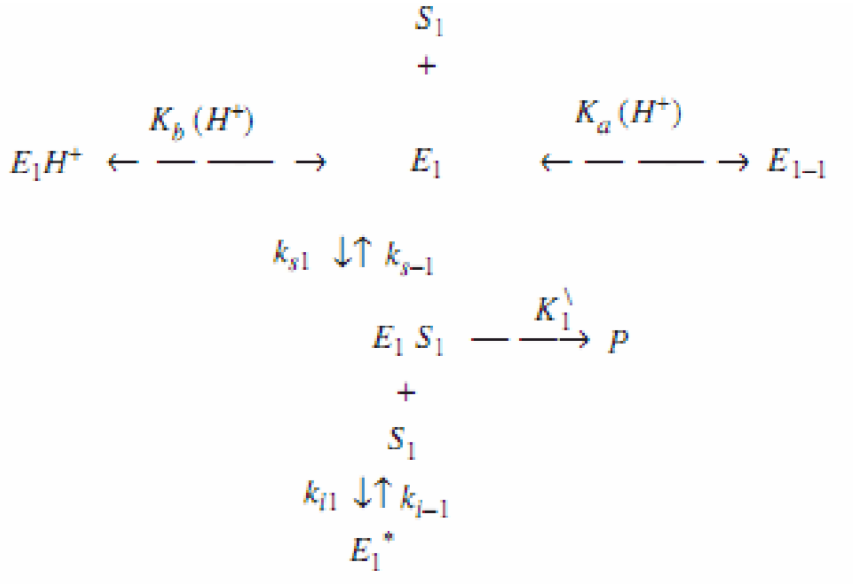

Figure 3.2: Hydrolysis Reaction Model

Hence, the reaction mechanism is inhibited by substrate. E_1, S_1, and E_1S_1 are related by:

$S_1\ E_1\ (K_{S1}) = k_{s-1}(E_1S_1)$

where $K_{S1} = k_{s-1}/k_{s1}$, E_1 and E^- related by:

$k_a(E_1) = k_{-a}E_1^-(H^+)$,

where $K_a = k_a/k_{-a}$, E_1 and EH_1^* are related by:

$k_b(E_1H^*) = k_{-b}(H^*)(E_1)$

$E_1H^* = k_{-b}/\ k_b\ (H^*)(E_1) = (H^*)(E_1)/\ K_b$

$K_b = k_{-b}/\ k_b$

$E_{t1} = E_1 + E^- + E_1H^+ = E_1(1 + K_a/H^+ + H^+/\ K_b) = K_{S1}/S_1(1 + K_a/H^+ + H^+/K_b)E_1S_1$

E_1^* is produced due to the inhibition by S_1, i.e.

$k_{i1}(E_1S_1)S_1 = E_1^*(k_{i-1})$

$E_1^* = k_{i1}(E_1S_1)S_1/\ k_{i-1} = (E_1S_1)S_1/K_{i1}$

letting $S_1 = S_{12}$ and $H^+ = H^+_2$ refer to ACh hydrogen ions concentrations in compartment (2), respectively, give

$E_t = E_{t1} + E_1S_1 + E_1^* = (E_1S_1)(K_{S1}/S_{12}(1 + K_a/H_2^+ + H_2^+/K_b) + 1 + S_{12}/ K_{i1})$

or $E_1S_1 = E_t(S_{12})/ S_{12} + K_{S1}(1 + K_a/H_2^+ + H_2^+/K_b) + S_{12}^2/ K_{i1}$

Therfore:

$R_2 = K_1(E_1S_1) = K_1E_t(S_{12})/ S_{12} + K_{S1}(1 + K_a/H_2^+ + H_2^+/K_b) + S_{12}^2/ K_{i1}$

By dividing through by (K_{S1}) and after some algebraic manipulations we get:

$R_2 = VM_2(s_{12})/ s_{12} + 1/h_1(h_2 + 1 + \delta h_2^2) + \alpha s_{12}^2$

Where $\delta = K_a/K_b$, $K_a = k_a/k_{-a}$, $K_b = k_b/k_{-b}$, $h = H^+/ K_a$, $s_{12} = S_{12}/ K_{S1}$, $\alpha = K_{S1}/ K_{i1}$

Therefore: $r2 = (s_{12})/ s_{12} + 1/h_1(h_2 + 1 + \delta h_2^2) + \alpha s_{12}^2$

3.3.2 MECHANISM OF HYDROLYSIS OF ACh IN COMPARTMENT 1

Figure 3.3 shows a full mechanism for the pH-dependent enzyme synthesis reaction model.

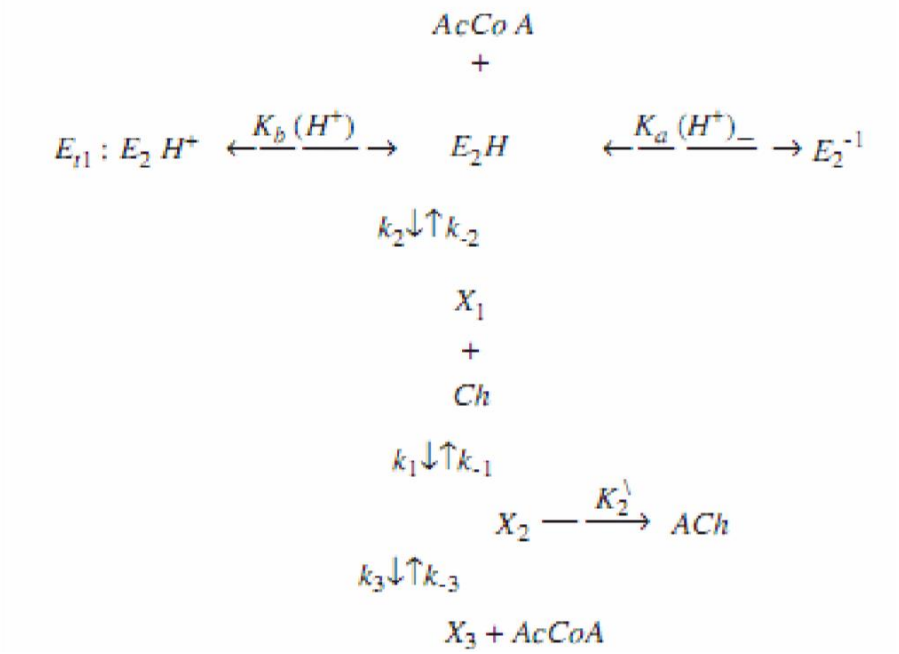

Figure 3.3: Synthesis reaction model

The full mechanism for the pH dependent ChAT kinetics is shown in Figure 3.3. The main reaction route occurs in the vertical direction. The active enzyme species exists in equilibrium with inactive protonated and de-protonated forms. The equilibria are driven by the pH of the system. E_2H, is the active form of the enzyme; E_2H^* and E_2^- are the protonated and de-protonated inactive enzyme forms. X_1, X_2, and X_3 are enzyme intermediate complexes.

The rate of synthesis can be written as:

$E_{t2} = E_2H_2^+ + E_2^- + E_2H = E_2H\ (1 + K_a/H_1^+ + H_1^+/ K_b)$

X_1 and X_2 are related through the following expressions:

$X_1(Ch)k_1 = X_2\ k_{-1}$, or $X_1 = k_{-1}/k_1(1/Ch)\ X_2 = K_1(1/Ch)\ X_2$

Where $K_1 = k_{-1}/k_1$, E_2H and X_2 are related by:

$k_2(AcCoA)\ E_2H = k_{-2}\ X_1(Ch)$ or $E_2H = K_1\ K_2\ X_2/\ AcCoA(Ch)$

where $K_2 = k_{-2}/\ k_2$

$E_{t2} = E_2H_1^+ + E_2^- + E_2H = K_1\ K_2\ X_2/\ AcCoA(Ch)\ (1 + K_a/H_1^+ + H_1^+/ K_b)$

X_2 and X_3 are related by

$X_2k_3 = X_3\ k_{-3}(AcCoA)$

$X_3 = X_2/(AcCoA)K_3$

$K_3 = k_{-3}/\ k_3$, Since $E_t = E_{t2} + X_1 + X_2 + X_3$ we get :

$E_t = X_2(K_1\ K_2\ /\ AcCoA(Ch)\ (1 + K_a/H_1^+ + H_1^+/ K_b) + K_1/(Ch) + 1 + (1/(AcCoA))K_3)$

Or

$X_2 = AcCoA(Ch)\ E_t/\ K_1\ K_2(1 + K_a/H_1^+ + H_1^+/ K_b) + K_1(AcCoA) + AcCoA(Ch) + Ch/\ K_3$

Since $R_1 = X_2\ K_2$, therefore :

$r_1 = \Theta_1\ s_{31}\ s_{21}/\ \Theta_2/h_1\ (h_1+1+\delta h_1^2) + \Theta_3\ s_{31} + \Theta_4\ s_{21} + \Theta_5\ s_{31}\ s_{21}$

Therefore; $r_2 = s_{12}/\ 1/h_2\ (h_2+1+\delta h_2^2) + s_{12} + \alpha\ s_{12}^2$

3.3.3 DYNAMIC MODEL EQUATIONS

The following equations depict the formulation of the dynamic model differential equations for the different components in the two compartments:

(A) The **Hydrogen ion** dynamic mole balances in the two compartments are given by

$V_j\ d[H^+]_j/dt = a_{1j}.q.(\ [H^+]_f - [H^+]_1\ ) - a_{2j}.\alpha'_{H^+}.A_M\ .(\ [H^+]_1 - [H^+]_2\ ) + V_j\ (a_{4j}.R_2.\overline{AChE} - R_{wj})$

for the indices j = 1, 2 which denote compartments 1 and 2 respectively. Here $a_{11} = a_{21} = a_{42} = 1$, $a_{12} = a_{41} = 0$, $a_{22} = -1$. $[H^+]_f$ is the concentration of hydrogen ions in the feed, and R_{wj} is the rate of water formation in compartment j.

(B) The **Hydroxyl ion** dynamic mole balances in the two compartments are given by

$V_j\ d[OH^-]_j/dt = a_{1j}.q.(\ [OH^-]_f - [OH^-]_1\ ) - a_{2j}.\alpha'_{OH^-}.A_M\ .(\ [OH^-]_1 - [OH^-]_2\ ) - V_j\ .R_{wj})$

(C) The **Acetylcholine** dynamic mole balances in the two compartments are given by

$V_j\ d[S_1]_j/dt = a_{1j}.q.([S_1]_f - [S_1]_1) - a_{2j}.\alpha'_{s1}.A_M.([S_1]_1 - [S_1]_2) + \overline{V_j}(a_{3j}.R_1.\overline{ChAT} - a_{4j}.R_2.AChE)$

(D) The **Choline** dynamic mole balances in the two compartments are given by

$V_j\ d[S_2]_j/dt = a_{1j}.q.([S_2]_f - [S_2]_1) - a_{2j}.\alpha'_{s2}.A_M.([S_2]_1 - [S_2]_2) + \overline{V_j}(-a_{3j}.R_1.\overline{ChAT} + a_{4j}.R_2.AChE)$

(E) The **Acetate** dynamic mole balances in the two compartments are given by

$V_j\ d[S_3]_j/dt = a_{1j}.q.([S_3]_f - [S_3]_1) - a_{2j}.\alpha'_{s3}.A_M.([S_3]_1 - [S_3]_2) + \overline{V_j}(-a_{3j}.R_1.\overline{ChAT} + a_{4j}.R_2.AChE)$

The pseudo steady state assumption for hydroxyl ions give us

$d[OH^-]/dt = 0$

Assuming that the hydrogen and hydroxyl ions are at equilibrium yields the equation

$K_w = [H^+]\cdot[OH^-]$

for K_w, the equilibrium constant of water reversible dissociation.

Subtracting equation (B) from equation (A) and substituting PSSH and into K_w equation (A) results in the equation

$V_j\ d[H^+]_j/dt = a_{1j}.q.([H^+]_f - [H^+]_1) - K_w.(1/[H^+]_f - 1/[H^+]_1) - a_{2j}.\alpha'_{H^+}.A_M.([H^+]_1 - [H^+]_2) + a_{2j}.A_M.\{\alpha'_{OH^-}.K_w.(1/[H^+]_1 - 1/[H^+]_2)\} + V_j(a_{4j}.R_2.AChE - R_{wj})$

All the above equations have been converted to its normalized form and are presented in Table 3.1. This gives a relatively simple two enzymes/two-compartments model which gives a set of eight coupled ordinary nonlinear differential equations. This system of Initial Value Problems has eight state variables $h_j(t)$, $s_{1j}(t)$, $s_{2j}(t)$, $s_{3j}(t)$ for j=1,2 that depend on the time t. These are computed with the help of normalized reaction rate $r_j(t)$. The system has 26 parameters that describe the dynamics for all compounds considered in the two compartments. Because of the lack of good experimental data in human brain chemistry, the presentation is limited to the use of carefully chosen normalized experimental parameters in order to reproduce the basic static and dynamic characteristics of this coupled enzymes system.

Most of the data is taken from earlier experimental work. The concentrations in the feed and reference values are taken from mouse and rat brain data for the sake of illustration. The membrane permeability parameters for s_2 and s_3 are assumed equal to the value for s_1. The normalized parameter B_1 is taken equal to B_2, which was found earlier experimentally. The

kinetic parameters θm for m =1,..,8 of reaction (1) are chosen by using a known dissociation constant and by keeping the experimentally found proportion for reaction (2) on substrate-inhibition and hydrogen-ion effects.

V_r	1.2
B_1	$5.033*10^{-5}$ kmol/m^3
B_2	$5.033*10^{-5}$ kmol/m^3
α_{H^+}	2.25
α_{OH^-}	0.5
α_{S1}	1
α_{S2}	1
α_{S3}	1
S_{1f}	2.4
S_{2f}	1.15
S_{3f}	3.9
α	0.5
γ	0.01
δ	0.1
K_{h1}	$1.0066*10^{-6}$ kmol/m^3
K_{s1}	$5.033*10^{-7}$ kmol/m^3
$[S_2]_{ref}$	0.0001 kmol/m^3
$[S_3]_{ref}$	0.000001 kmol/m^3
Θ_1	32000
Θ_2	4
Θ_3	0.125
Θ_4	0.125
Θ_5	84500
Θ_6	65
Θ_7	76.72
Θ_8	0.00769

Table 3.2: 26 experimentally obtained numerical parameter values

3.4 FORMULATION OF THE INTERACTION BETWEEN β-AMYLOID PEPTIDES AND ChAT KINETICS THROUGH 2E2C MODEL

The ACh neurocycle is shown in Figure 1.1 where the presynaptic neuron represents the plant for ACh synthesis where it contains the enzyme ChAT, choline, and acetyl CoA. The presynaptic neuron is considered as compartment 1 while both synaptic cleft and postsynaptic neuron represent compartment 2. It is observed that choline is the only component produced from the hydrolysis which is recycled to compartment 1 and re-used for ACh synthesis. ACh and acetyl-CoA are synthesized in compartment 1. Figure 3.1 shows a simple form of the feedback model of ACh cholinergic neurocycle shown in Figure 1.1. Every compartment is considered a constant volume and isothermal continuous stirred tank reactor (CSTR) with a constant flow rate and constant recycle ratio. Also, the two compartments are separated by a permeable membrane. β-amyloid peptides interact with ChAT inside compartment 1. There is a strong relation between β-amyloid peptides and cholinergic dysfunction which is one of the main symptoms of Alzheimer disease (AD). Furthermore, β-amyloid could inhibit the activity of the enzyme ChAT leading to reduction in the levels of ACh and memory impairment. ChAT activity could be completely reduced significantly with β-amyloid.

3.5 MODEL ASSUMPTIONS: EFFECTS OF β-AMYLOID INHIBITION

All assumptions made for investigating the effect of β-amyloid:

1) The presynaptic of cholinergic nerve terminal is described by compartment 1. Inside this compartment ACh is synthesized by the reaction of choline and acetyl CoA in the presence of catalytic effect of ChAT enzyme.

2) Postsynaptic of neurons together with synaptic cleft are considered as compartment two. Both postsynaptic and synaptic cleft are unified to be in one compartment instead of two or three because both of them are harmonized and interactive and also to simplify the calculations in solving the model particularly when the dimensionality is too high.

3) Both compartments are assumed to be divided with a permeable membrane.

4) The internal masses transfer in compartment one between synaptic vesicles and cytoplasm and in compartment two between ACh and postsynaptic receptors are neglected because every compartment is assumed to be a homogenous

5) All matters in the presynaptic neuron are transported to the postsynaptic cleft via passive diffusion where all concentrations in compartment 1 should be higher than that in compartment 2; however, choline uptake from the postsynaptic cleft to the presynaptic

neurons is performed by facilitated diffusion via high affinity choline uptake transporters, (HACUTs).

6) It is observed that concentrations of all state variables in compartment two are the average of concentrations in postsynaptic and synaptic cleft.

7) Temperature is considered constant where the system is assumed to be isothermal and there is no effect for any temperate changes on the system.

8) Transport of β-amyloid from compartment 1 to compartment 2 is neglected. To justify, it is noted that transport of β-amyloid from compartment 1 to compartment 2 is by passive diffusion and the transport rate is extremely lower than that from the cytoplasm to compartment 1. The latter transport (from cytoplasm to compartment1) addresses the blood brain barriers (BBB) according to saturable mechanism such as Monod and Michaelis-Menten kinetics.

9) The initial concentration of β-amyloid is assumed to be zero.

10) Feed stream rate to compartment one and outlet flow from compartment two are considered to be constant with a value of q (m^3/sec).

3.6 COMPETITIVE INHIBITION OF ChAT IN 2E2C Model

ChAT and AChE are the two cholinergic enzymes considered in the 2E2C model. ChAT is responsible for synthesis of ACh in compartment 1 of the 2E2C model, while AChE catalyzes the degradation of ACh in compartment 2. It is found that incorporation of β-amyloid into rat brains in vivo and at nano to pico molar concentrations, shows significantly a decrease in ChAT activity and ACh production.

This finding suggests that β-amyloid may act as a general modulator of ChAT enzyme activity leading to a reduction in ACh synthesis. The exact mechanisms of ChAT modulation by β-amyloid are still currently unknown. It is possible that β-amyloid aggregates may directly inhibit ChAT activity by competitively binding to active sites, or perhaps limit the activity of secondary proteins responsible for ChAT synthesis and regulation. Since level of intracellular ChAT is generally maintained at a concentration much higher than that of the reactants for ACh production, modification of the 2E2C model to incorporate inhibition of ChAT activity is required to understand the mechanisms of the interaction between ChAT and β-amyloid aggregates. To examine the phenomenon of ChAT activity inhibition by β-amyloid in a simpler model, βamyloid is considered to act directly as a competitive inhibitor of ChAT enzyme.

Figure 3.4 illustrates a modified version of pH-dependent enzyme synthesis reaction model used in the two enzyme/two compartment model. The modification (represented in square brackets) takes into account two possible pathways in which β-amyloid may bind competitively to intermediate complexes, thereby inhibiting their ability to progress to the main reaction direction (in the vertical pathway) towards ACh synthesis. In such case β-amyloid may bind directly to the active form of the enzyme E_2H to generate the inactive E_2H [bA] complex (Figure 3.4 (a)), thus limiting the availability of active enzymes to carry out ACh synthesis and decrease net enzyme activity. Similarly, it is also possible that β-amyloid may bind to the enzyme intermediate complex X_2 thereby preventing ACh release from the complex (Figure 3.4 (b)). The generation of β-amyloid is modeled by adding another differential equation identical to that of choline leakage hypothesis. However, note that the leakage term was not incorporated into the choline differential equation for compartment 1. The accumulation of Aβ is described as follows:

$db/dT = K_{L2} - K_{L3}(S_{11}) - K_{L4}.b$

where the term (K_{L2}) describes the generation of Aβ aggregates from amyloid precursor protein, the term ($-K_{L3}(S_{11})$) describes the impact of ACh levels in the presynaptic neuron on the rate of formation of Aβ aggregates and the term ($-K_{L4}.b$) represents the reduction in Aβ aggregates levels due to the enzymatic hydrolysis and diffusion in the neuronal membranes.

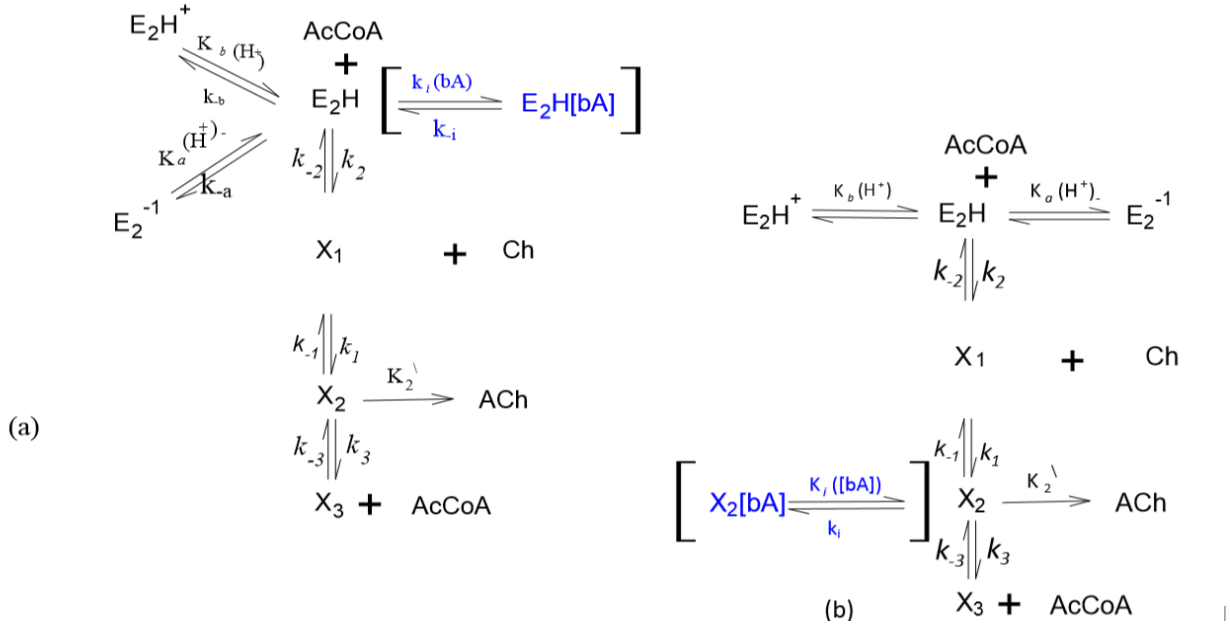

Figure 3.4: Possible competitive inhibition mechanisms for β-amyloid ([bA]) during pH-dependent ChAT synthesis of ACh (areas of inhibition are displayed in square brackets). The reaction route occurs in the vertical direction. E_2H is the active form of the enzyme; E_2H^+ and E_2^{-1} are the protonated and de-protonated inactive forms. X_1, X_2 and X_3 are enzyme intermediate complexes. a) β-amyloid competitively binds to active enzyme complex E_2H; b) β- amyloid competitively binds to enzyme intermediate X_2.

3.6.1 KINETIC MECHANISM 1

COMPETITIVE INHIBITION OF Aβ WITH ALL SPECIES ACTIVATED ENZYME COMPLEX E_2H

The synthesis rate for competitive inhibition of β- amyloid with activated enzyme complex E_2H can be derived as follows:

$X_1(Ch)k_1 = X_2k_{-1}$

Or $X_1 = X_2\ K_1/(Ch)$,

Where $K_1 = k_{-1}/\ k_1$

By the assumption of rapid equilibrium, E_2H and X_1 can be related by

$k_2\ (AcCoA)\ E_2H = k_{-2}\ X_1$

or $E_2H = K_1\ K_2\ X_2/(AcCoA)\ (Ch)$,

where $K_2 = k_{-2}/\ k_2$

By rapid equilibrium assumption, $E_2H[Aβ]$ complex can be expressed as

$k_i\ E_2H[A\beta] = k_{-i}\ E_2H[A\beta]$

or $E_2H[A\beta] = K_i\ E_2H[A\beta]$

where $K_i = k_i / k_{-i}$

From the ionization of E_2H,

$E_2H(H^+)\ k_{-b} = E_2\ H^+\ k_b$

Or $E_2H^+ = E_2H(H^+)/\ K_b$

From the deionization of E_2H,

$E_2^-(H^+)\ k_a = E_2\ H^+\ k_{-a}$

$E_2^- = E_2H\ K_a/(H^+)$

From the above equations we get

$E_{t2} = E_2H + E_2^- + E_2H_1^+ + E_2H[A\beta]$

$= K_1\ K_2\ X_2/(AcCoA)\ (Ch)*\{1 + K_a/H^+ + H^+/\ K_b + A\beta.K_i\}$

Where X_2 and X_3 are related by

$X_3 = X_2/K_3(AcCoA)$

Where $K_3 = k_{-3}/\ k_3$

$E_t = E_{t2} + X_1 + X_2 + X_2$

$E_t = K_1\ K_2\ X_2/(AcCoA) *\{1 + K_a/H^+ + H^+/\ K_b + A\beta.K_i\} + K_1\ X_2/(Ch) + X_2 + X_2/K_3(AcCoA)$

$X_2= E_t(AcCoA)\ (Ch)/\ K_1\ K_2(1 + K_a/H^+)+H^+/\ K_b+A\beta.K_i +K_1(AcCoA)+/(AcCoA)(Ch)+(Ch)/K_3$

$h_1 = H_1^+/\ K_a$

$$X_2= \frac{E_t(AcCoA)(Ch)*(S_{2ref}\ S_{3ref})^{-1}}{\{K_1K_2(1+1/\ h_1+h_1\ (K_a/\ K_b)+A\beta.K_i)+K_1(AcCoA)+(AcCoA)(Ch)+(Ch)/K_3\}*(S_{2ref}\ S_{3ref})^{-1}}$$

$$X_2= \frac{E_t(AcCoA)\ (Ch)*(S_{2ref}\ S_{3ref})^{-}}{\{\frac{K_1K_2}{h_1}(1+h_1+h_1^2(K_a/K_b)+\frac{A\beta}{A\beta_{ref}}(h_1.A\beta_{ref}.K_i))+K_1(AcCoA)+(AcCoA)(Ch)+(Ch)/K_3\})*(S_{2ref}\ S_{3ref})^{-1}}$$

$X_2 = E_t\ (S_{31}\ S_{21})/(\Theta_2/h_1(1+h_1+\delta h_1^2+h_1.(1+A\beta K_{i1})\ )+\Theta_3.s_{31}+\ \Theta_4.s_{21} + \Theta_5.s_{21}.\ s_{31}$

Since $r_1 = K_2^{'}X_2$

$r_1 = \Theta_1\ (S_{31}\ S_{21})/(\Theta_2/h_1(1+h_1+\delta h_1^2+h_1.(1+A\beta K_{i1})\ )+\Theta_3.s_{31}+\ \Theta_4.s_{21} + \Theta_5.s_{21}.\ s_{31}$

Where Aβ is the generated β-amyloid concentration in the dimensionless form and K_i is the dimensionless equilibrium rate constant for the first proposed inhibition mechanism (Figure 3.4 (a)). Table 3.3 summarizes the nine ordinary-differential equations of 2E2C model considering ChAT-inhibition effect by β-amyloid based on the previous kinetic mechanism (1), and Table 3.4 gives the values of kinetic parameters.

3.6.2 KINETIC MECHANISM 2

COMPETITIVE INHIBITION OF β-AMYLOID AGGREGATES WITH ENZYME INTERMEDIATE COMPLEX X_2

In this kinetic mechanism, there is a competitive inhibition of β-amyloid with enzyme intermediate complex X_2. During ACh synthesis as shown in (Figure 3.4 (b)), the modified rate equation can be derived as shown below.

X_1 and X_2 are related through the following expressions:

$X_1(Ch)k_1 = X_2\ k_{-1}$

Or $X_1 = K_1\ X_2/Ch$,

Where $K_1 = k_{-1}/\ k_1$

By the assumption of rapid equilibrium, E_2H and X_1 can be related by:

$K_2 = k_{-2}/\ k_2$

From the ionization of E_2H

$E_2H(H^+)k_{-b} = E_2H^+k_b$

Or $E_2H^+ = E_2H(H^+)/K_b$

From the deionization of E_2H

$E_2^-(H^+)k_a = E_2H.k_{-a}$

$E_2^- = E_2H.K_a/(H^+)$

From the above equations we get

$E_{t2} = E_2H + E_2^- + E_2H^+$

$= X_2K_2K_1/(AcCoA)(Ch)\ \{1+ K_a/(H^+) + (H^+)/K_b\}$

X_2 and X_3 are related by

$X_3 = X_2/K_3(AcCoA)$

Where $K_3 = k_{-3}/k_3$

Also

$k_i\ X_{22}[A\beta] = k_{-i}\ X_2[A\beta]$

$X_2[A\beta] = K_i\ X_{22}[A\beta]$

$K_i = k_i/k_{-i}$

$E_t = X_2K_2K_1/(AcCoA)(Ch)\ \{1+ K_a/(H^+) + (H^+)/K_b\} + K_1\ X_2/Ch+ X_2/K_3(AcCoA)+X_2+ K_i[A\beta]$

$$X_2 = \frac{(AcCoA)(Ch)\ E_t}{K_2K_1\{1+ K_a/(H^+) + (H^+)/K_b\}+ K_1(AcCoA)+(AcCoA)(Ch)+ Ch/K_3+ K_i[A\beta]\ (AcCoA)(Ch)}$$

$R_1 = K_2'\ X_2$

$$r_1 = \frac{\Theta_1.S_{21}.S_{31}}{\Theta_2/h_1(h_1+1+\delta\ h_1^2)+ \Theta_3S_{31}+\Theta_4S_{21}+\Theta_5\ S_{21}\ S_{31}(1+K_{I1}\ A\beta)}$$

Where Aβ is the concentration of generated β-amyloid in the dimensionless form and K_{I1} is the dimensionless equilibrium rate constant for the second proposed inhibition mechanism shown in Figure 3.4 (b). In the next section, the results presented are based on the previous equation of r_1 replacing that r_1 in Table 3.3 while all other equations remain the same as the kinetic parameter values in Table 3.4

3.6.3 KINETIC MECHANISM 3

NON-COMPETITIVE INHIBITION OF β-AMYLOID AGGREGATES WITH ALL SPECIES ChAT

β-amyloid inhibitor behaves as a non-competitive inhibitor and could attack all ChAT species in the synthesis reaction in compartment 1 with the same affinity if the reaction follows either a rapid equilibrium random mechanism or an ordered sequential. Figure 4.16 shows the kinetic mechanism 3 for the synthesis reaction catalyzed by ChAT where all species in ChAT can be exposed to β-amyloid peptide, where E = ChAT, I = βamyloid, A = Choline, B = Acetyl-coA. In the same way as the previous kinetic mechanisms 1 and 2 were derived, the final form of the rate of ACh synthesis derived is shown as below:

$$r_1 = \frac{\Theta_1 . S_{21} . S_{31}}{(\Theta_2/h_1(h_1+1+\delta\, h_1^2)+ \Theta_3 S_{31}+\Theta_4 S_{21}+\Theta_5\, S_{21}\, S_{31})(1+K_{I1}\, A\beta)}$$

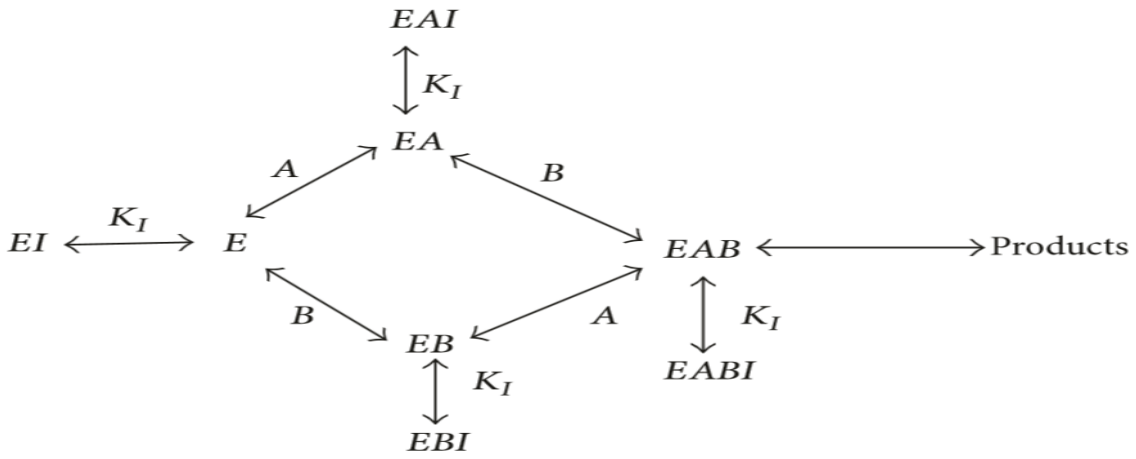

Figure 3.5: Possible noncompetitive inhibition mechanisms for *β*amyloid aggregates during pH-dependent ChAT synthesis of ACh: E = ChAT, I =*β*-amyloid aggregates, A = choline, B = acetyl-coA, and Products=ACh.

An eight-dimension non-linear mathematical (two-enzyme/two-compartment) model is developed for a coupled ChAT/AChE enzyme system where the physiological phenomena of the choline uptake from the synaptic cleft to the presynaptic neuron and fully ionization of acetic acid assumption are considered. Three different kinetic mechanisms explaining the interaction between β- amyloid aggregates and ChAT activity are suggested and tested through the incorporation of the rate of ACh synthesis where ChAT activity is inhibited by β-amyloid into the 2E2C model. The reduction in ChAT activity is one of the symptoms of brains with AD. In the first kinetic mechanism, β- amyloid aggregates attack activated enzyme complex E_2H. In the second kinetic mechanism a competitive inhibition of β-amyloid aggregates occurs with enzyme intermediate complex X_2. In the third kinetic mechanism, β-amyloid aggregates attack all species in ChAT enzyme. The effect of three bifurcation parameters on the system performance have been investigated. These bifurcation parameters are: hydrogen ions feed concentrations, AChE activity, and β-amyloid aggregates. The results of bifurcation diagrams for the system were obtained using MATLAB, software for ordinary differential equations. The complex static and dynamic phenomena such as bifurcation, oscillatory, instability and chaotic behavior of the system are extensively investigated with comparison to the actual physiological values to predict and control the system performance.

Item	Compartment	Differential equation
Hydrogen protons	1	$\frac{dh_{(1)}}{dT} = h_f - \gamma_1\left(\frac{1}{h_f}\right) - \alpha_H\left(h_{(1)} - h_{(2)}\right) + \alpha_{OH}\gamma_1\left(\frac{1}{h_{(1)}} - \frac{1}{h_{(2)}}\right)$
	2	$\frac{dh_{(2)}}{dT} = V_R(\alpha_H(h_{(1)} - h_{(2)}) - \alpha_{OH}\gamma_1\left(\frac{1}{h_{(1)}} - \frac{1}{h_{(2)}}\right) - \left(h_{(2)} - \frac{\gamma_1}{h(2)}\right) + \frac{B_2}{k_{h1}}r(2))$
Acetylcholine	1	$\frac{ds_{1(1)}}{dT} = s_{1f} - \alpha_{s1}\left(s_{1(1)} - s_{1(2)}\right) + \frac{B_1 r(1)}{K_{s1}} - K_{bA}\, s_{1(1)}\, bA$
	2	$\frac{ds_{1(2)}}{dT} = V_R(\alpha_{S_1}\left(s_{1(1)} - s_{1(2)}\right) - s_{1(2)} - \frac{B_2 r(2)}{K_{s1}})$
Choline	1	$\frac{ds_{2(1)}}{dT} = s_{2f} + R^* s_{2(2)} - \alpha_{S2_1}\left(s_{2(1)} - s_{2(2)}\right) - \frac{B_1}{S_{2reference}}r(1)$
	2	$\frac{ds_{2(2)}}{dT} = V_R(\alpha_{S2}\left(s_{2(1)} - s_{2(2)}\right) - (1+R)^* s_{2(2)} + \frac{B_2}{S_{2reference}}r(2))$
Acetate	1	$\frac{ds_{3(1)}}{dT} = s_{3f} - \alpha_{S3}\left(s_{3(1)} - s_{3(2)}\right) - \frac{B_1}{S_{3reference}}r(1)$
	2	$\frac{ds_{3(2)}}{dT} = V_R(\alpha_{S3}\left(s_{3(1)} - s_{3(2)}\right) - s_{3(2)} + \frac{B_2}{S_{3reference}}r(2))$
β- amyloid aggregates	1	$\frac{dbA}{dT} = K_{L_2} - K_{L_3}\, s_{1(1)} - K_{L_4}\, bA$
Rate of synthesis ($r_{(1)}$)	1	$r_1 = \frac{\theta_1 s_{21} s_{31}}{(\theta_2 / h_1(h_1 + 1 + \delta h_1^2)(1 + K_{I1}\, bA) + \theta_3 s_{31} + \theta_4 s_{21} + \theta_5 s_{21} s_{31})}$
Rate of hydrolysis ($r_{(2)}$)	2	$r(2) = \frac{s_{12}}{s_{12} + 1/h_2(h_2 + 1 + \delta h_2^2) + \alpha s_{12}^2}$

Table 3.3: Dimensionless forms of the ordinary differential equations of ChAT inhibition effects by β-amyloid aggregates of kinetic mechanism

Parameter	Value
Θ_1	5.2
Θ_2	12
Θ_3	1000
Θ_4	5
Θ_5	1
α	0.5
δ	1
K_{h1}	$1.066*10^{-6}$ kmol/m^3
K_{s1}	$5.033*10^{-7}$ kmol/m^3
S_{2ref}	0.0001 kmol/m^3
S_{3ref}	0.00001 kmol/m^3
B_1	$5.033*10^{-5}$ kmol/m^3
B_2	$5.033*10^{-5}$ kmol/m^3
α_{H^+}	2.25
α_{OH^-}	0.5
α_{S1}	1.5
α_{S2}	1.5
α_{S3}	1
V_r	1.2
h_f	8.2
S_{1f}	15
S_{2f}	1.15
S_{3f}	3.9
γ	0.01
R	0.8
K_{bAref}	20nm/L
K_{L2}	Assumed
K_{L1}	$3*K_{L2}$
K_{L3}	$0.035*K_{L2}$
K_{L4}	$0.176*K_{L2}$
K_{i1}	10.015
K_{bA1}	0.05

T_{ref}	0.1h
$A\beta_{ref}$	20nm/L

Table 3.4: Values of the kinetic parameters

4. RESULTS AND DISCUSSIONS

(A) FEED HYDROGEN ION CONCENTRATION (h_f)

The feed hydrogen ions concentration is expressed as the dimensionless value h_f when it is used as a bifurcation parameter and the corresponding value of the pH feed will be given in ACh region; while the hydrogen ions concentration is reported as a state variable in terms of pH. The feed hydrogen ions are defined as the hydrogen ions coming to the nerve ending as a product of metabolic reactions occurring outside the presynaptic terminal. For example, the metabolic synthesis of acetyl CoA and metabolic reactions associated with ATP produce hydrogen ions. The concentrations of these feed hydrogen ions (hf) will influence pH of the ACh neurocycle. h_f is an independent bifurcation parameter and will be investigated.

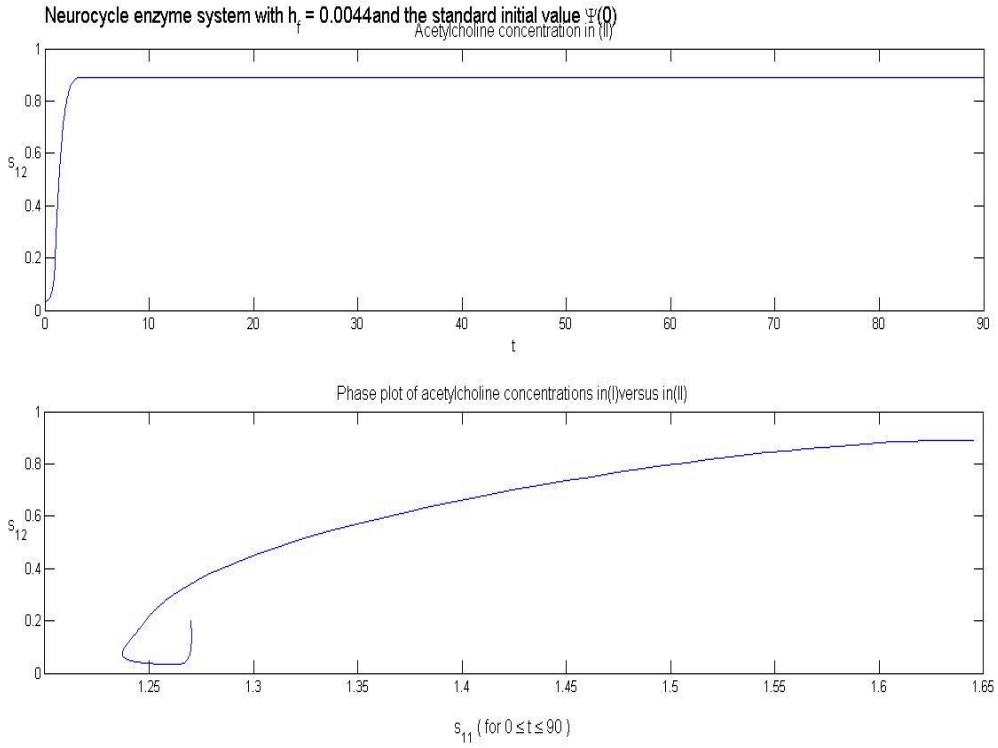

Figure 4.1: Profile of $s_{12}(t)$ and phase plot of s_{12} versus s_{11}; Convergence to a fixed steady state, no periodicity

For all values hf $\leq$ 0.0044, the plots have the same shape as displayed in Figure 4.1. Note that the phase plot starts out from the end of the lower left hook and proceeds toward the upper right in the bottom image as t increases.

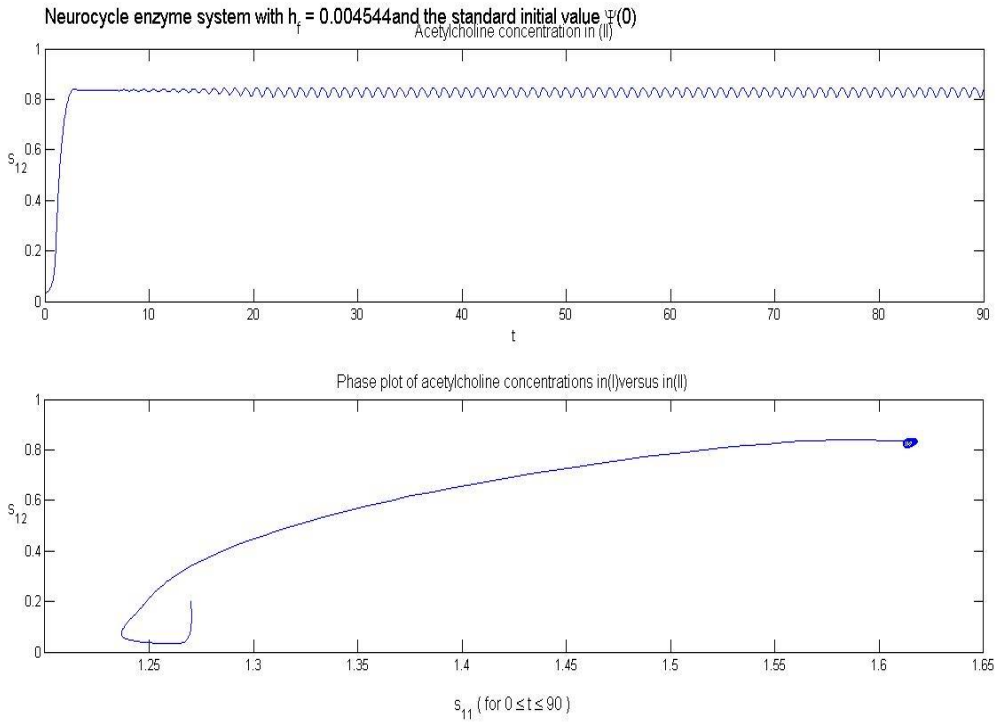

Figure 4.2: Profile of $s_{12}(t)$ and phase plot of s_{12} versus s_{11}; Increasing oscillatory behavior with a single period

When we increase h_f, small but increasing oscillations of the concentration profiles occur, as the following plots for $h_f = 0.004544$

For $h_f = 0.004546$, the solution $s_{12}(t)$ becomes more irregular at first until it settles into one stable limit cycle; see Figure 4.3.

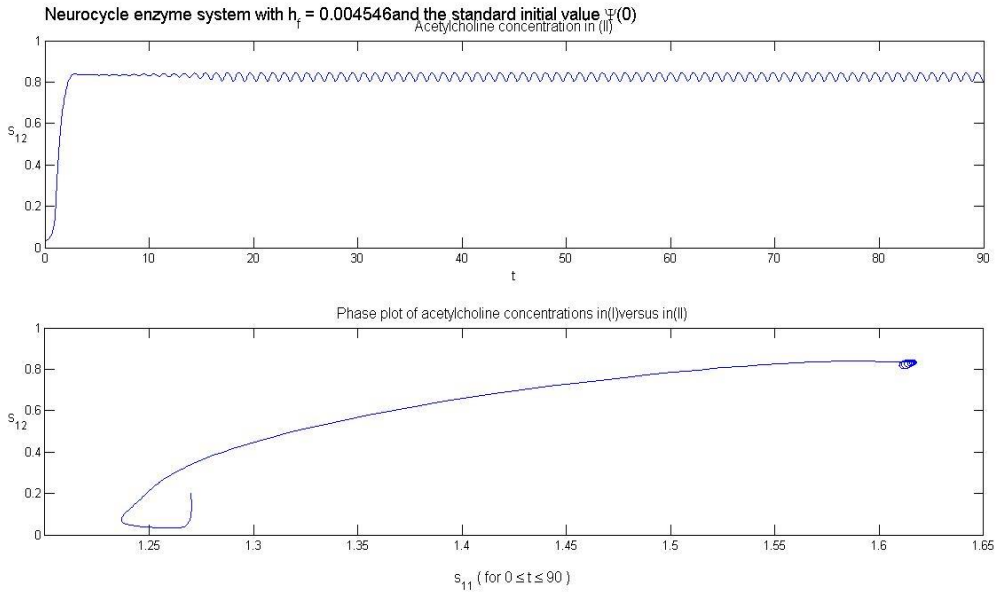

Figure 4.3: Profile of $s_{12}(t)$ and phase plot of s_{12} versus s_{11}; larger-amplitude single-period limit cycle

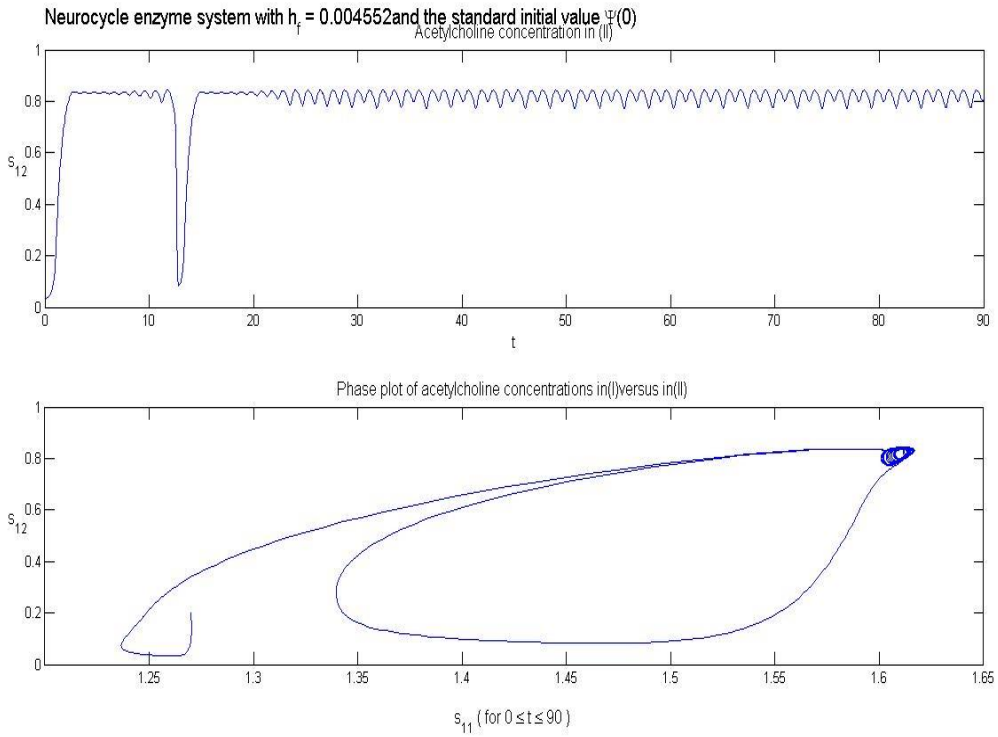

Figure 4.4: Profile of $s_{12}(t)$ and phase plot of s_{12} versus s_{11}; Larger-amplitude single period with a one double-loop limit cycle

Our next-higher value of h_f =0 .004552 exhibits a double-loop limit cycle, or a period two periodic attractor in the phase plot of Figure 4.4

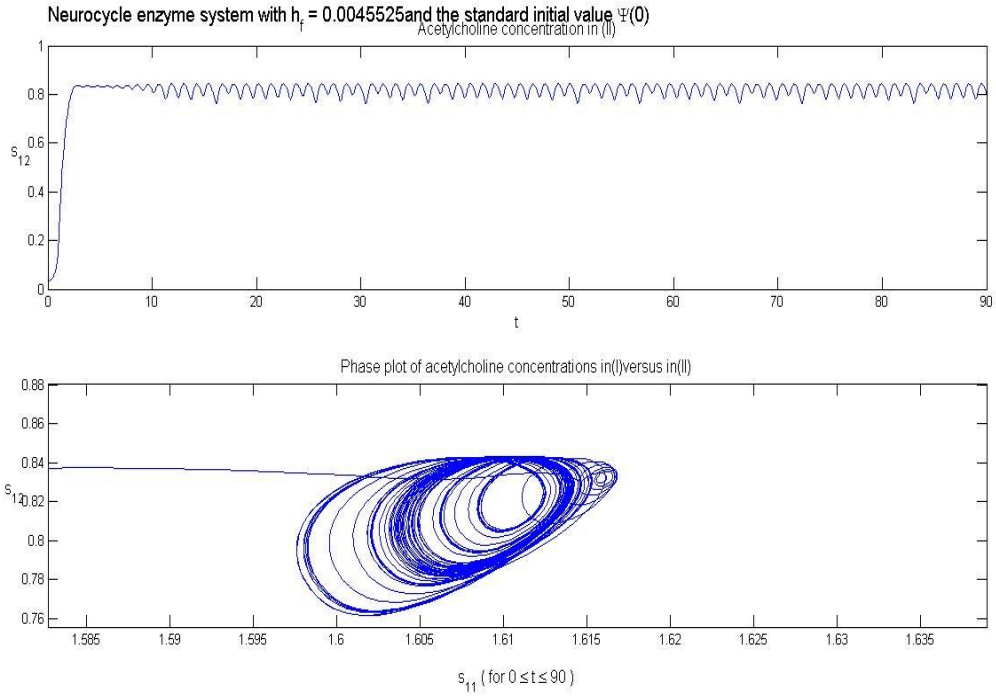

Figure 4.5: Profile of $s_{12}(t)$ and phase plot of s_{12} versus s_{11}; chaotic behavior

If we increase h_f further to 0.0045525, we observe chaotic behavior of the $s_{12}(t)$ concentration in Figure 4.5. This also manifests itself in the phase plot, which consists of random loops until our plotting ends at 90 time units. The profile and phase plots show oscillatory behavior of Figure 4.5, but no pattern or periods can be seen therein. This is called a strange attractor in modern nonlinear dynamics theory. A strange attractor can be chaotic or non-chaotic (high-dimensional torus).

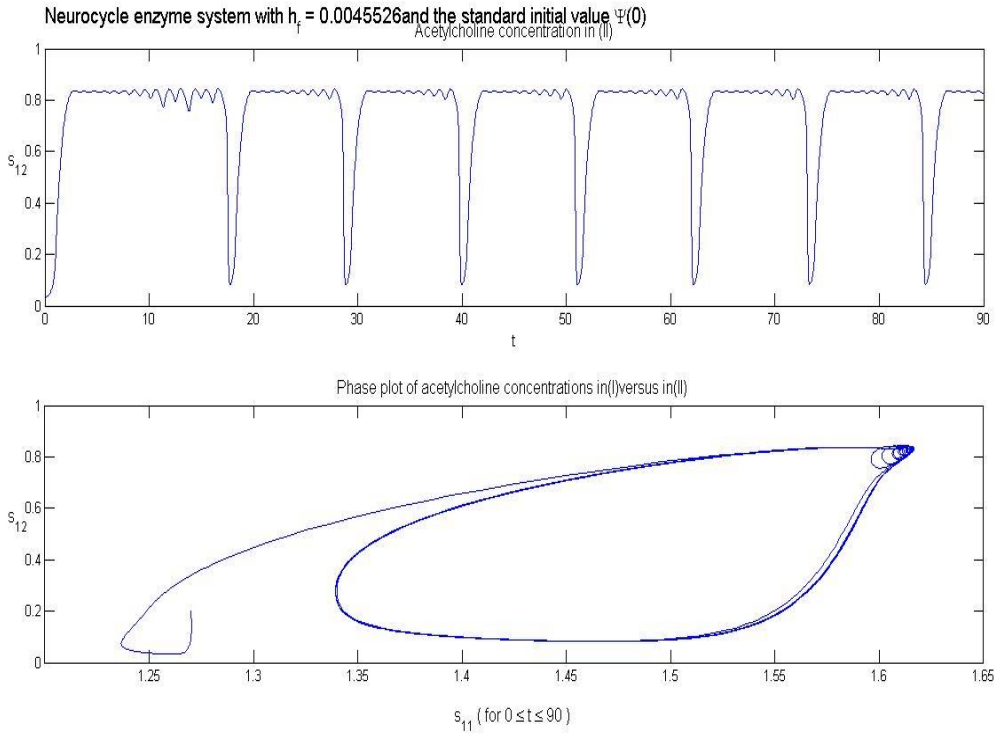

Figure 4.6: Profile of $s_{12}(t)$ and phase plot of s_{12} versus s_{11}; after a short period of chaos, periodic behavior begin

A slight increase to h_f =0 .0045526 ends the chaotic behavior after around 20 time units, and an orderly 9-periodic behavior (period-nine periodic attractor) sets in for the solution from then on, as seen in Figure 4.6.

When h_f =0 .0045539, the initial chaotic behavior has stopped and the system's limit cycle is reached on the second pass through a large-amplitude drop in the acetylcholine concentration in compartment (II), as shown in Figure 4.7. In Figure 4.7 we count 10 separate periods of mostly increasing amplitudes until the cycle repeats.

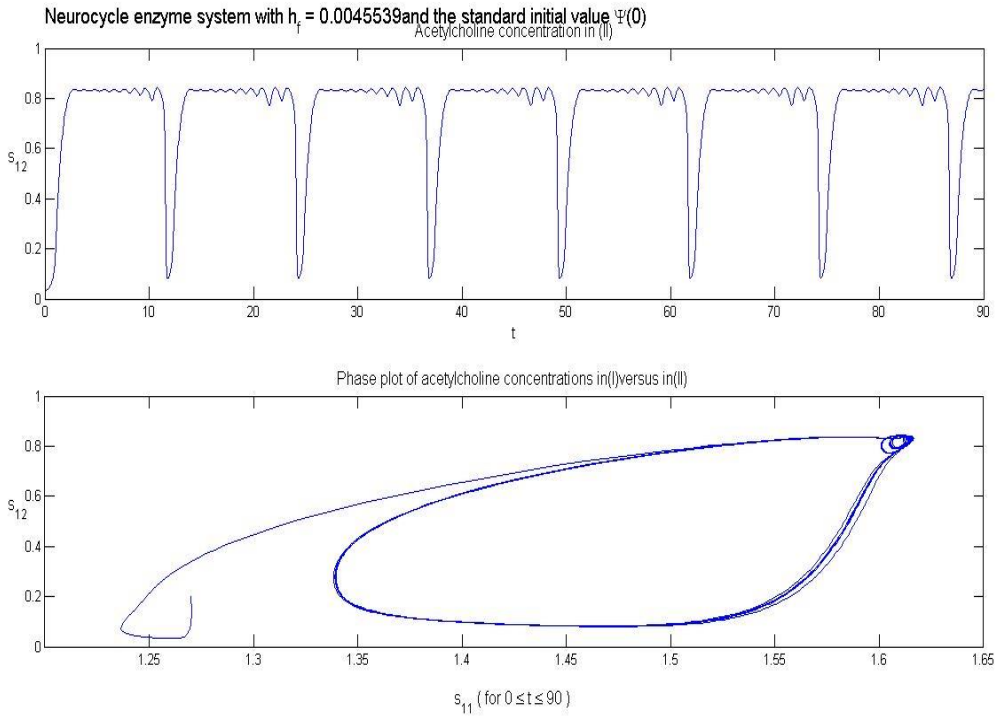

Figure 4.7: Profile of $s_{12}(t)$ and phase plot of s_{12} versus s_{11}; 10-periodic limit cycle

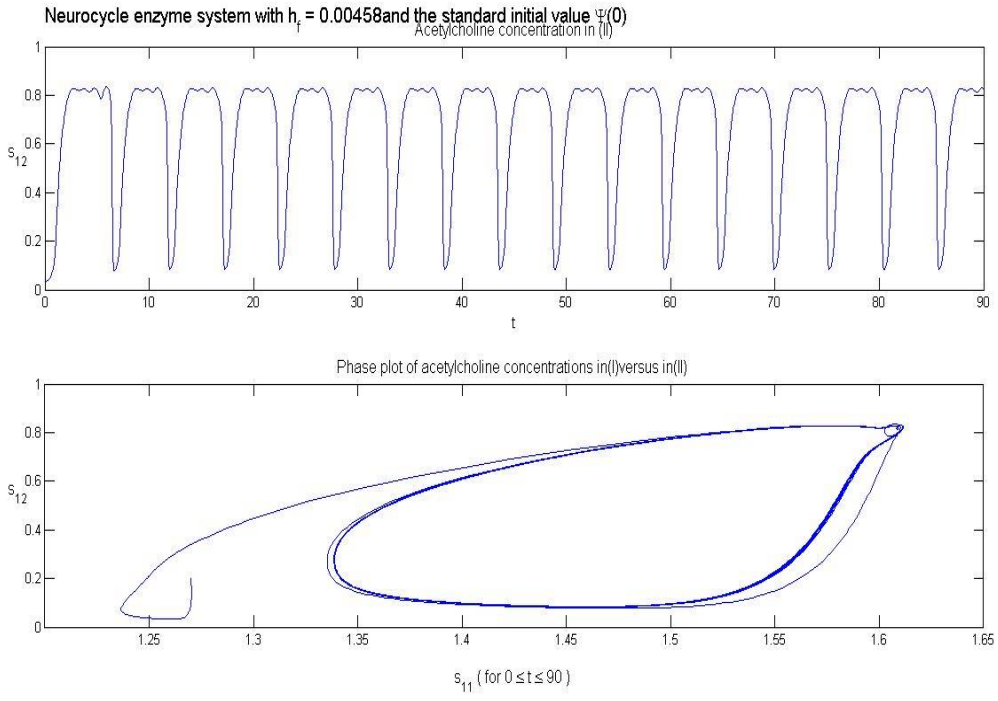

Figure 4.8: Profile of $s_{12}(t)$ and phase plot of s_{12} versus s_{11}; 3-periodic limit cycle

The graph for h_f =0 .00458 that generates a 3-periodic limit cycle (period-three periodic attractor).

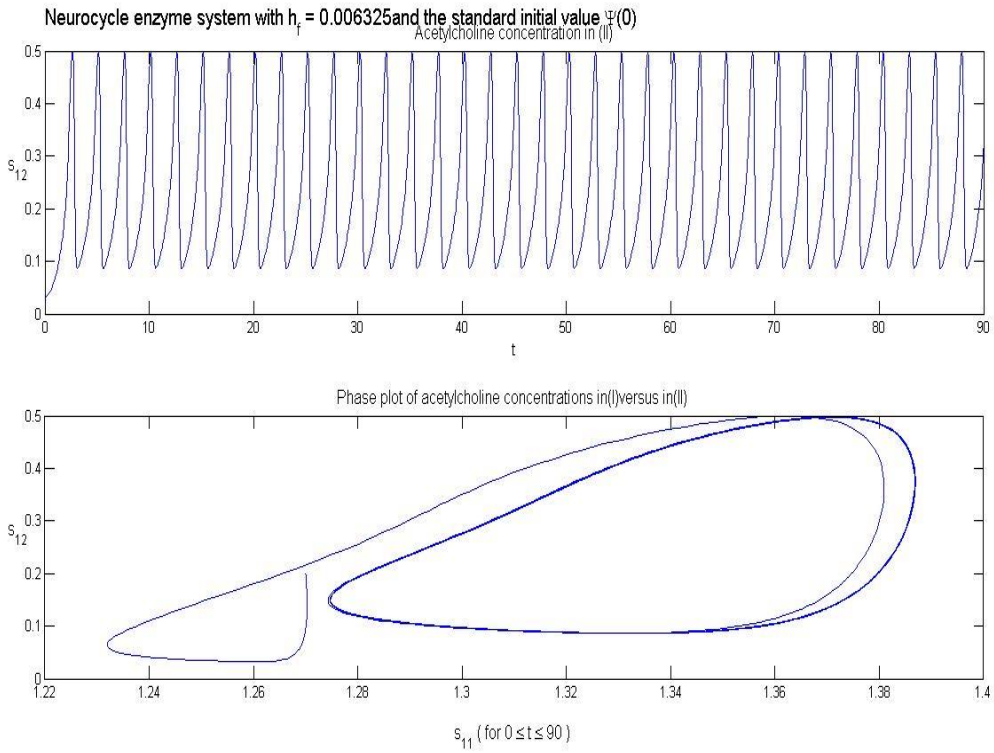

Figure 4.9: Profile of $s_{12}(t)$ and phase plot of s_{12} versus s_{11}; single periodic limit cycle

For much larger h_f values such as h_f =0 .006325, the limit cycle has exactly one maximum, and this is reached after the first complete cycle, as shown in Figure 4.9. For even larger values of h_f, the system eventually reaches a unique fixed steady state that is stationary and involves no limit cycle at all, just as we have seen to be the case for small values of h_f in Figure 4.1.

For h_f =0 .0065, the phase plot starts at s_{11} =1 .27 and s_{12} =0 .2 in the bottom plot of Figure 4.10 and moves in two spiral loops toward the asymptotic steady state with $s_{11} \approx 1.285$ and $s_{12} \approx 0.17$, as depicted in Figure 4.10. Figure 4.11 depicts a unified eight profile plot veriying the assertion that the system reaches a unique fixed steady state when h_f = 0 .0065.

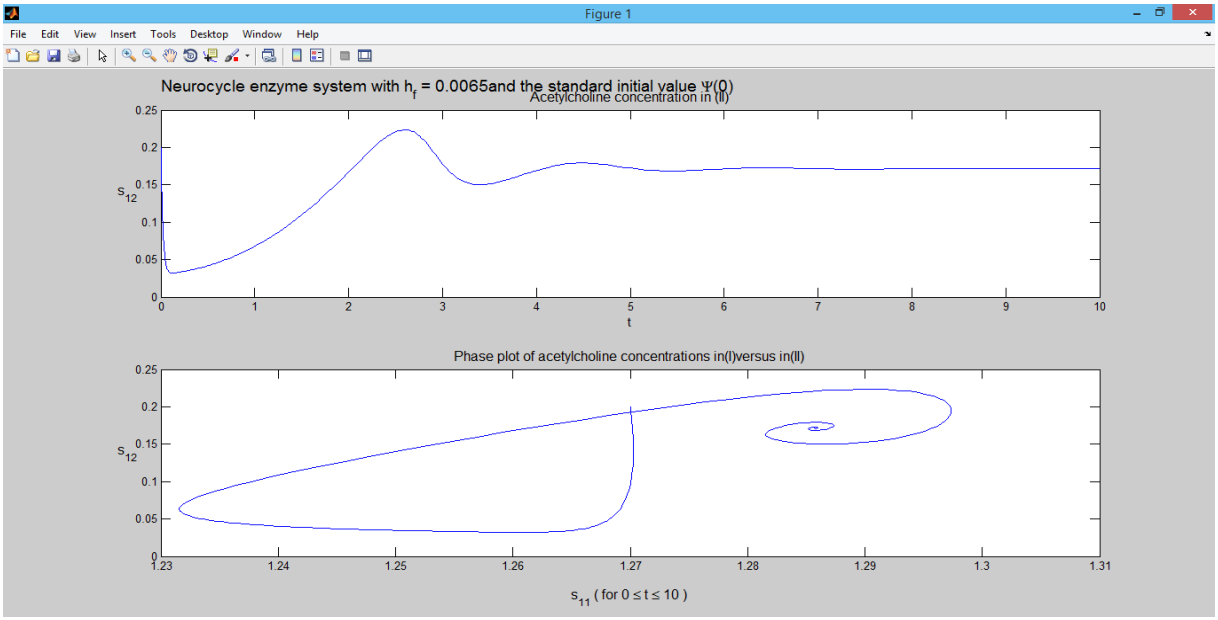

Figure 4.10: Profile of $s_{12}(t)$ and phase plot of s_{12} versus s_{11}; a unique steady state for large h_f values

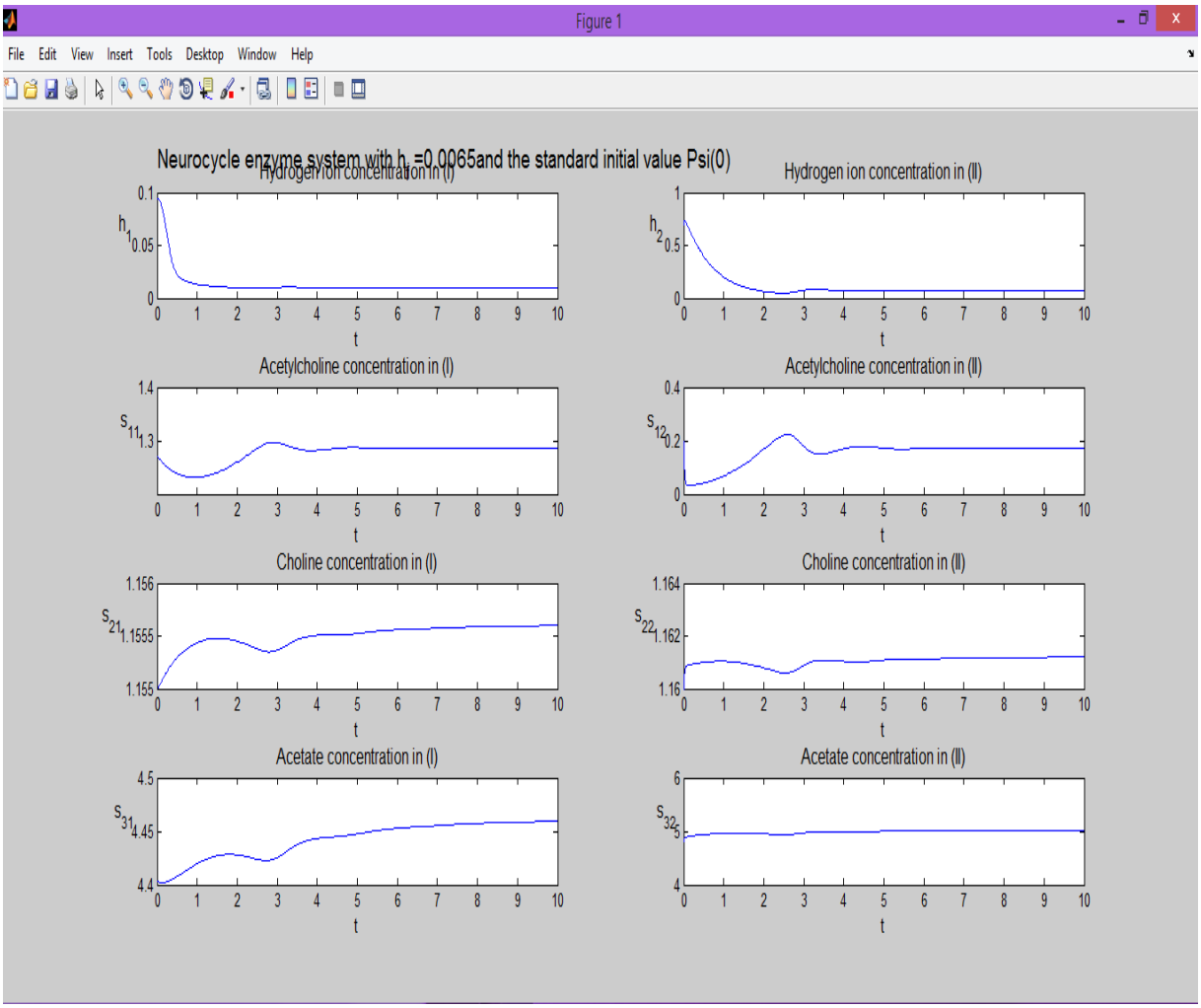

Figure 4.11: Complete set of profiles

B) <u>AChE ENZYME ACTIVITY</u>

AChE enzyme is the enzyme responsible for the hydrolysis of ACh in compartment (2) into choline and acetate after the interaction between ACh and postsynaptic receptors. It is involved in the nervous transmission. Therefore; it is very important to investigate the effect of the activity of AChE enzyme (B_2) on the ACh neurocycle system. The parameter B_2 is chosen for this in order to gain some insight into possible consequences of varying the capability of the acetylcholinesterase to hydrolyze the neurotransmitter. Imbalances in this capability give rise to devastating diseases such as Alzheimer's and Parkinson's. The enzyme activity is included in the grouped parameter B_2, which includes the maximum reaction velocity in reaction 2. The parameter B_2 itself includes the enzyme activity together with three constants for the enzyme system, namely the concentration of acetylcholinesterase in compartment (2), the volume V_2 of compartment (2), and the flow rate q.

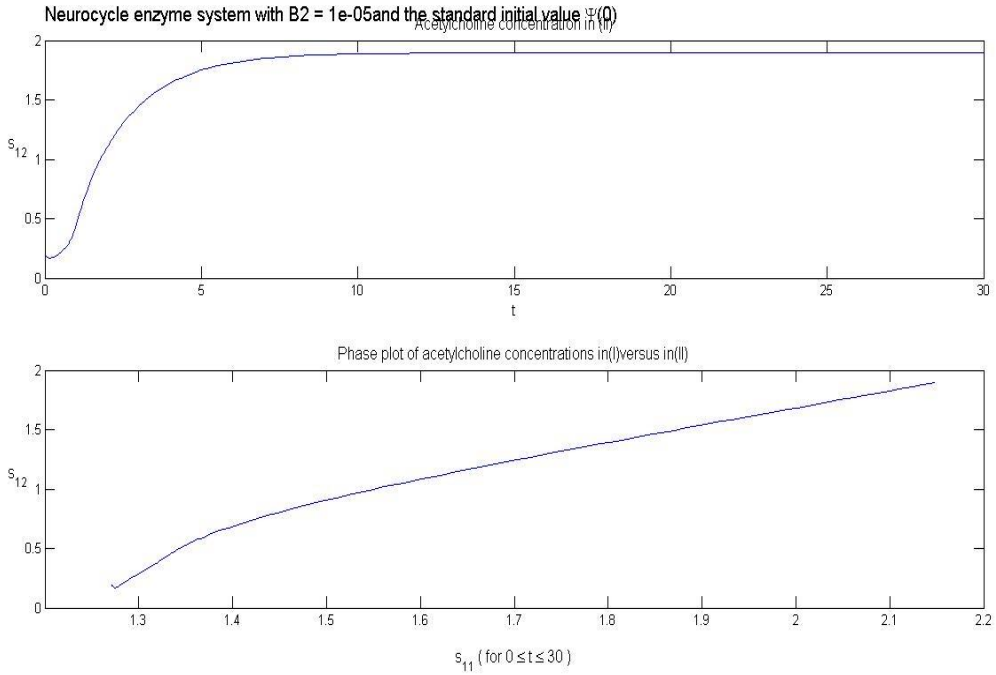

Figure 4.12: Profile of $s_{12}(t)$ and phase plot of s_{12} versus s_{11}; $B_2 = 0.00001$

Starting with $B_2 = 0.00001$ s_{12} rises to a value of 1.9 and attains steady state at this value. The phase plot attains a linear behavior at $s_{11} = 1.4$

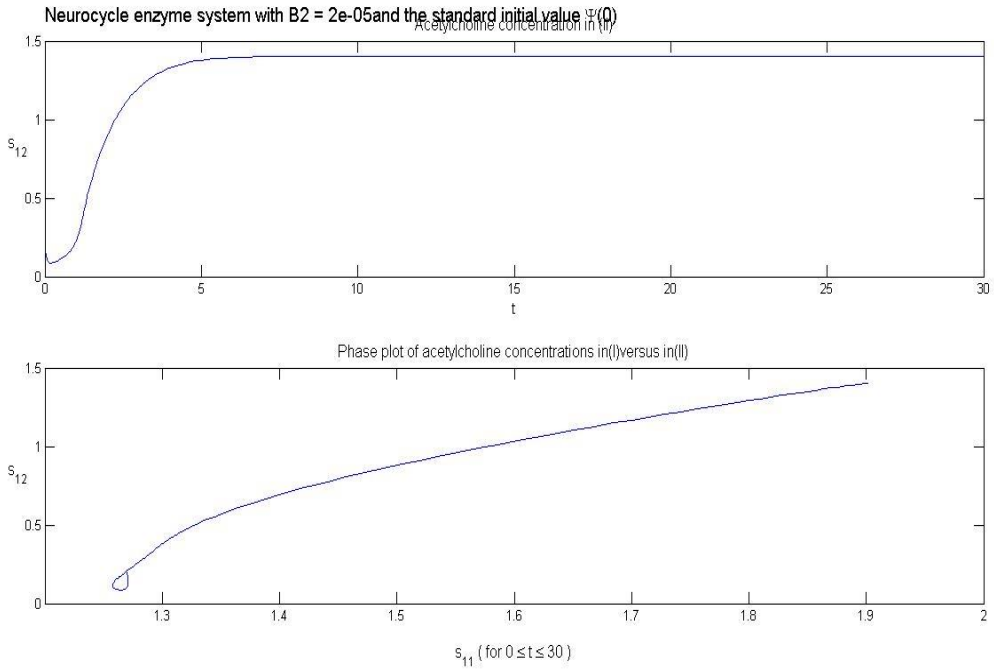

Figure 4.13: Profile of $s_{12}(t)$ and phase plot of s_{12} versus s_{11}; $B_2 = 0.00002$

At $B_2 = 0.00002$ s_{12} attains steady state at a lower value of 1.4. The phase plot consists of a single loop.

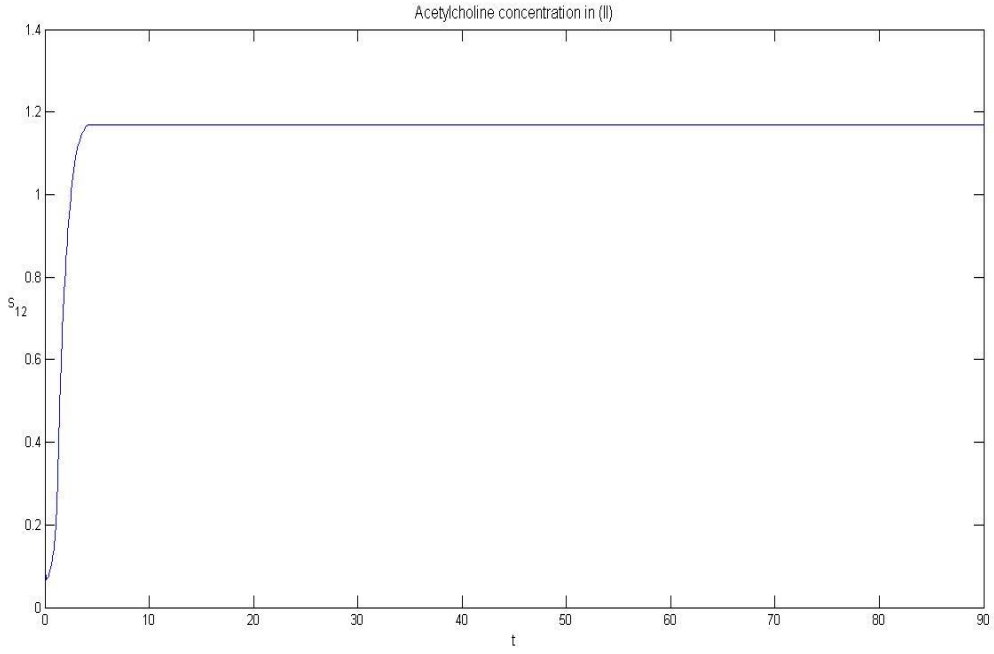

Figure 4.14: Profile of $s_{12}(t)$ and phase plot of s_{12} versus s_{11}; $B_2 = 0.000025$

At $B_2 = 0.000025$ s_{12} attains steady state at the value of 1.19. The curve has a sharp bend at this value.

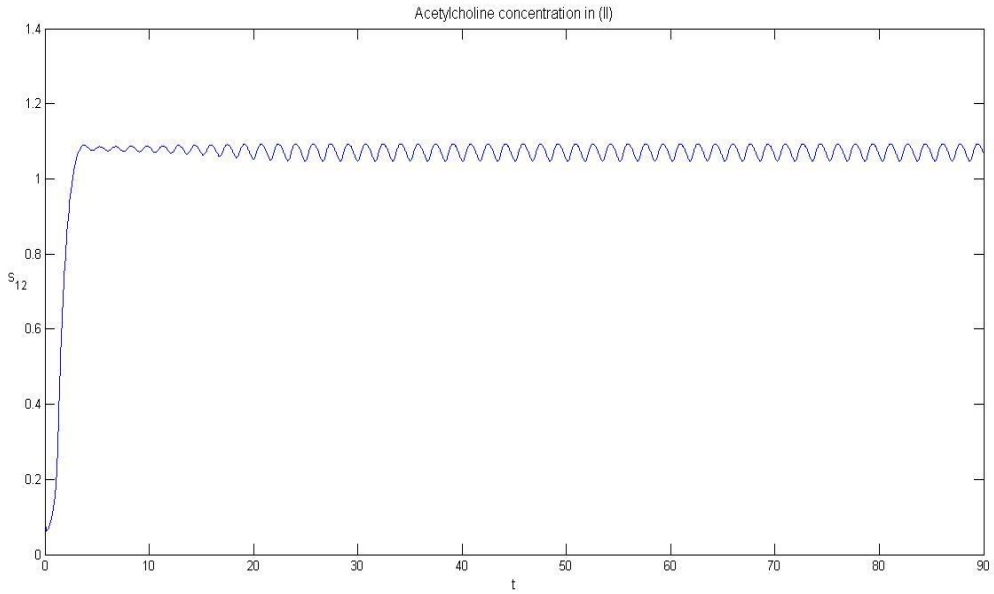

Figure 4.15: Profile of $s_{12}(t)$ and phase plot of s_{12} versus s_{11}; $B_2 = 0.000027$

The value of $B_2 = 0.000027$ marks the onset of the oscillatory behavior of s_{12}.

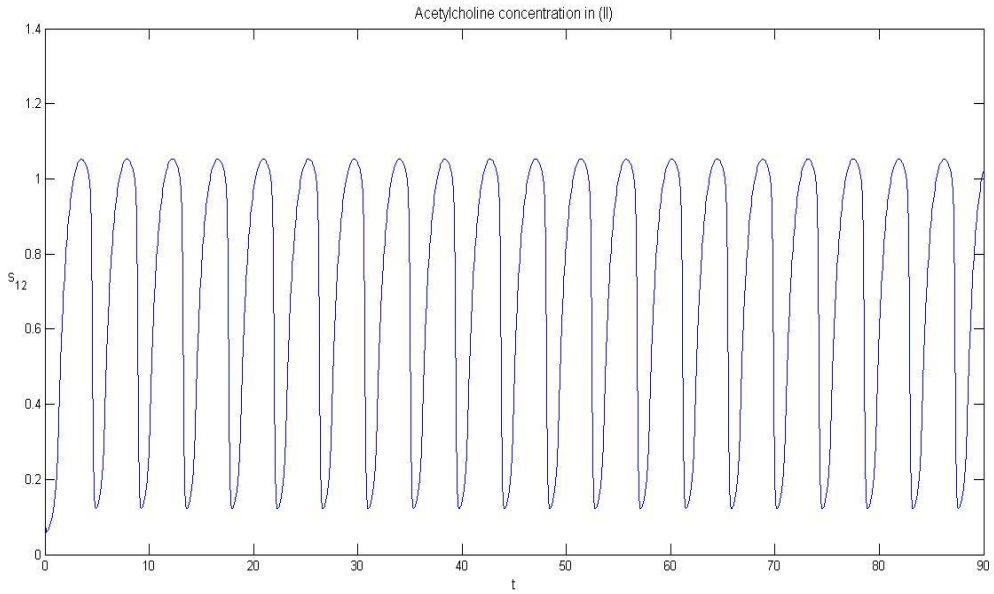

Figure 4.16: Profile of $s_{12}(t)$ and phase plot of s_{12} versus s_{11}; $B_2 = 0.000028$

At $B_2 = 0.000028$, s_{12} continues to showcase a behavior of one-period limit cycle with a decreased amplitude.

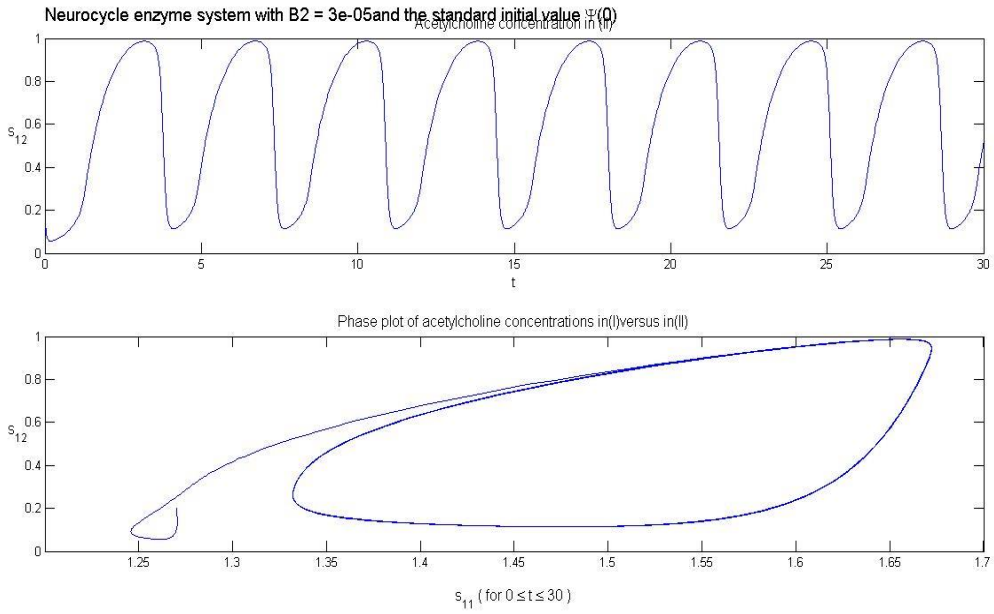

Figure 4.17: Profile of $s_{12}(t)$ and phase plot of s_{12} versus s_{11}; $B_2 = 0.00003$

At $B_2 = 0.00003$ s_{12} exhibits a limit cycle of amplitude 1. The phase plot twists into multiple loops, each one corresponding to one small bump of the profile of $s_{12}(t)$.

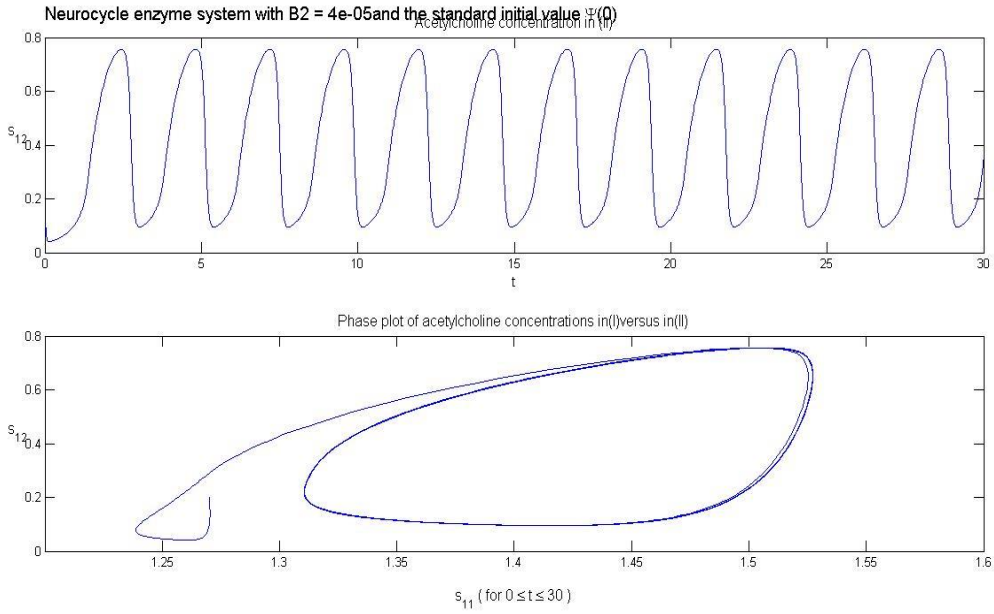

Figure 4.18: Profile of $s_{12}(t)$ and phase plot of s_{12} versus s_{11}; $B_2 = 0.00004$

At $B_2 = 0.00004$ s_{12} exhibits a limit cycle of increased frequency and lower amplitude.

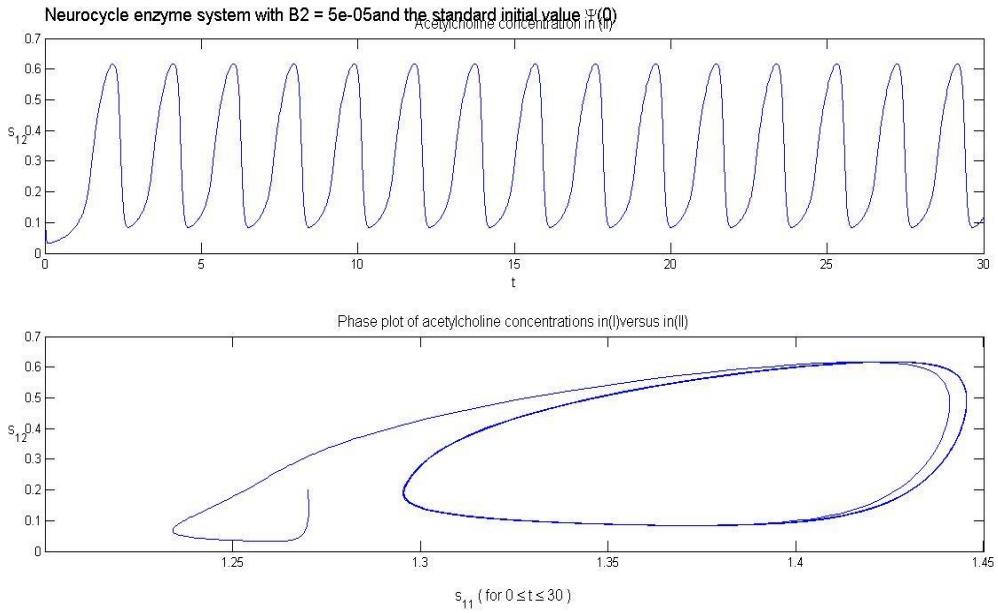

Figure 4.19: Profile of $s_{12}(t)$ and phase plot of s_{12} versus s_{11}; $B_2 = 0.00005$

At $B_2 = 0.00005$ s_{12} continues the previous trend. The phase starts out from the end of the lower left hook which becomes broader in this plot and proceeds toward the upper right in the bottom image as t increases.

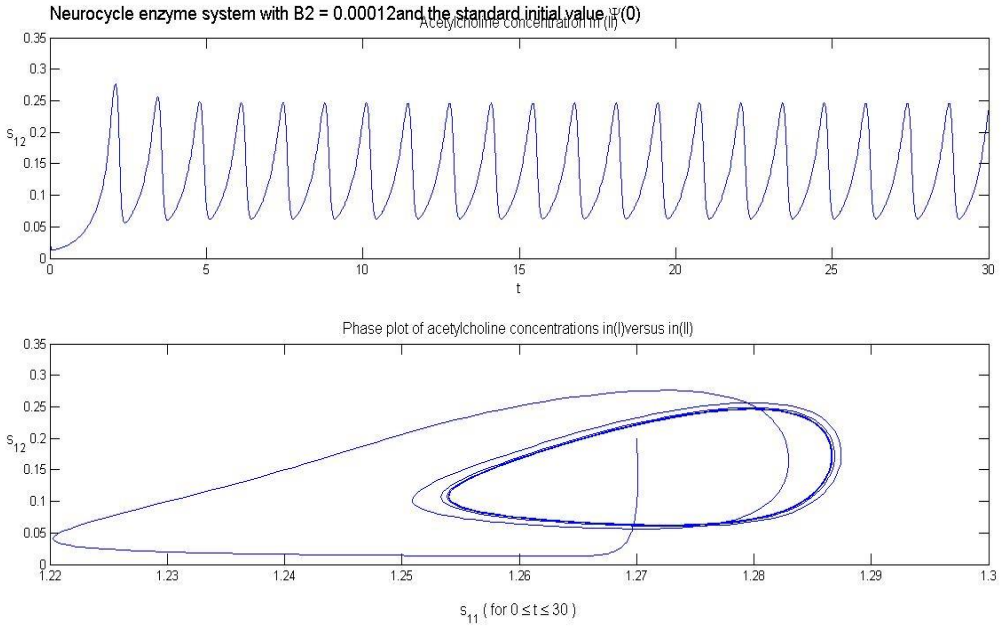

Figure 4.20: Profile of $s_{12}(t)$ and phase plot of s_{12} versus s_{11}; $B_2 = 0.00012$

At $B_2 = 0.00012$ s_{12} starts taking sharper turns after reaching the amplitude value.

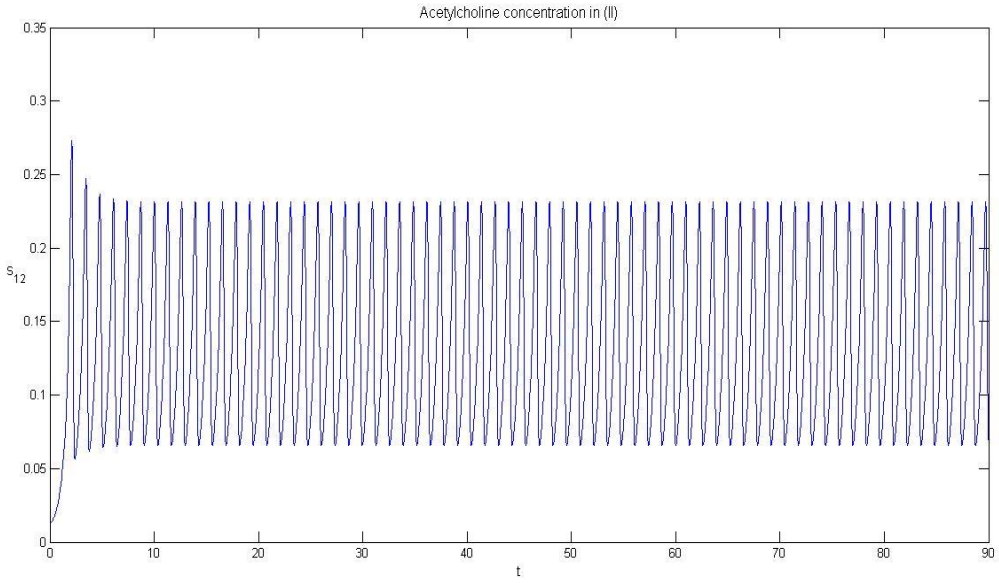

Figure 4.21: Profile of $s_{12}(t)$ and phase plot of s_{12} versus s_{11}; $B_2 = 0.000121$

At $B_2 = 0.000121$ s_{12} exhibits a limit cycle of variable value of the first and second amplitude. The amplitudes become constant after the third limit cycle.

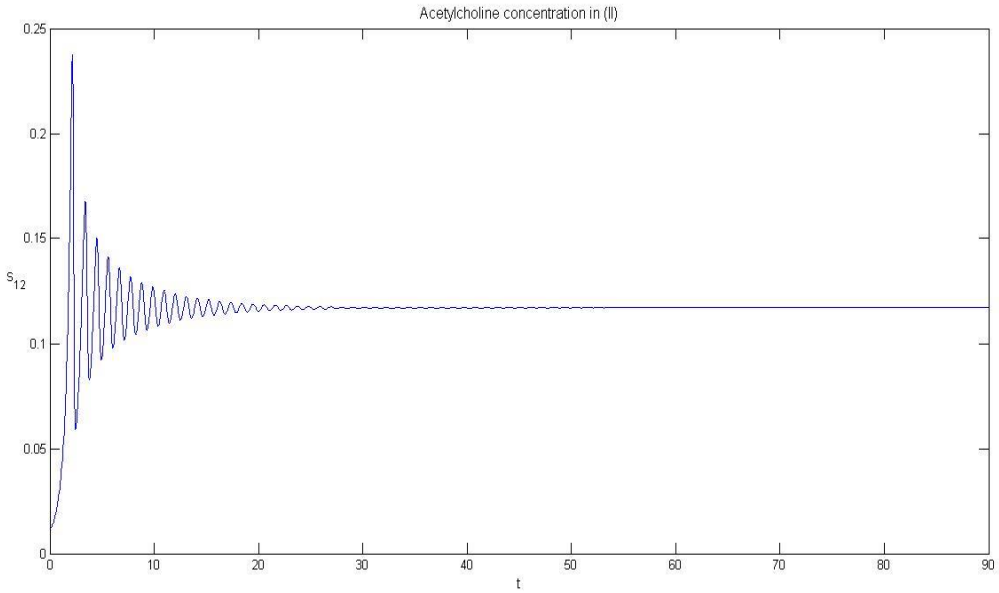

Figure 4.22: Profile of $s_{12}(t)$ and phase plot of s_{12} versus s_{11}; $B_2 = 0.000129$

At $B_2 = 0.000129$ s_{12} exhibits an oscillatory behavior which finally attains steady state after 30 time units.

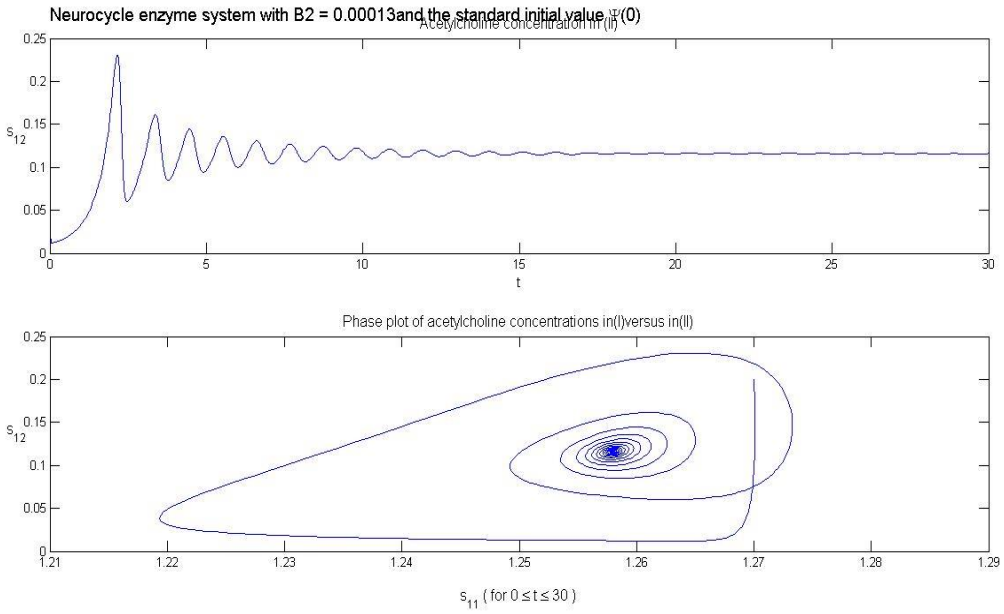

Figure 4.23: Profile of $s_{12}(t)$ and phase plot of s_{12} versus s_{11}; $B_2 = 0.00013$

At $B_2 = 0.00013$ s_{12} exhibits an oscillatory behavior in the beginning which lasts till 15 limit cycles.

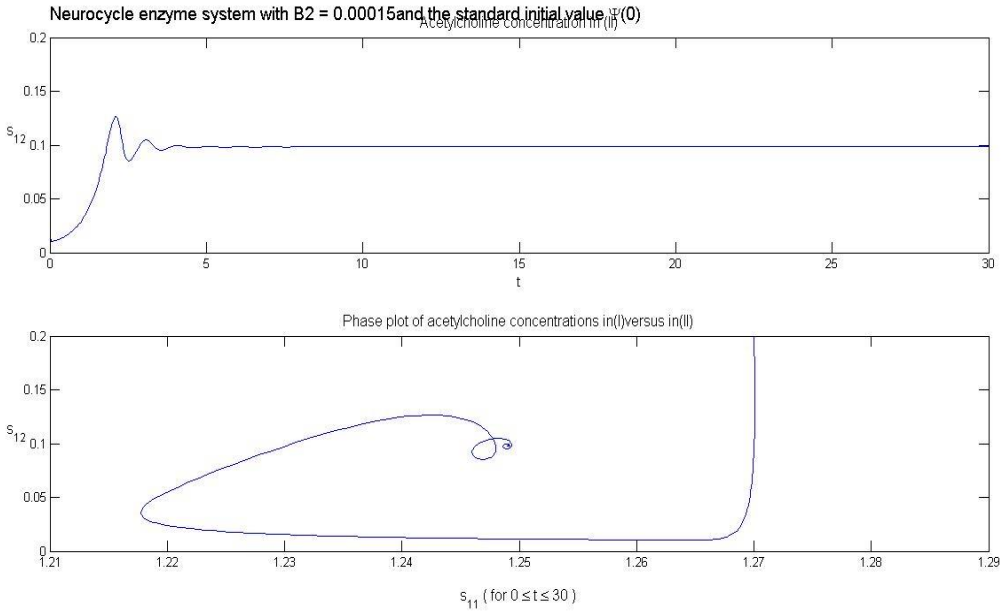

Figure 4.24: Profile of $s_{12}(t)$ and phase plot of s_{12} versus s_{11}; $B_2 = 0.00015$

At $B_2 = 0.00015$ s_{12} exhibits an oscillatory behavior in the beginning which lasts till 3 limit cycles and attains a steady state at the value of 0.1

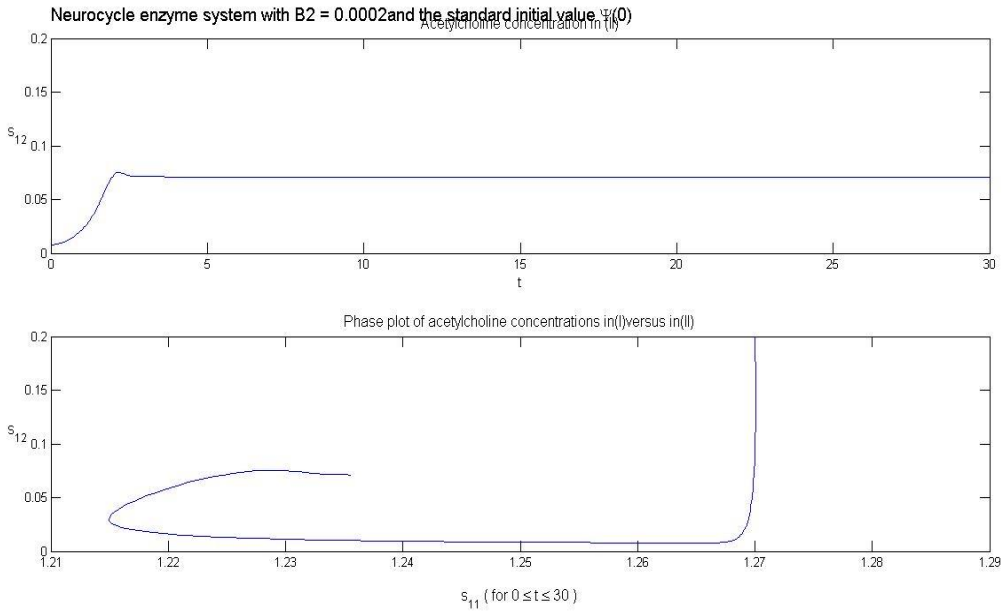

Figure 4.25: Profile of $s_{12}(t)$ and phase plot of s_{12} versus s_{11}; $B_2 = 0.00020$

At $B_2 = 0.00020$ s_{12} attains a steady state behavior at a lower value.

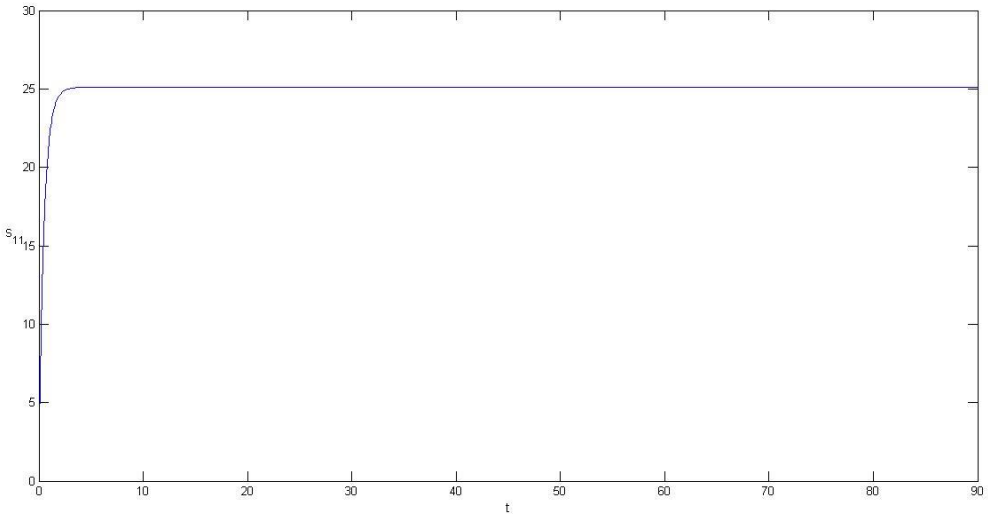

(a)

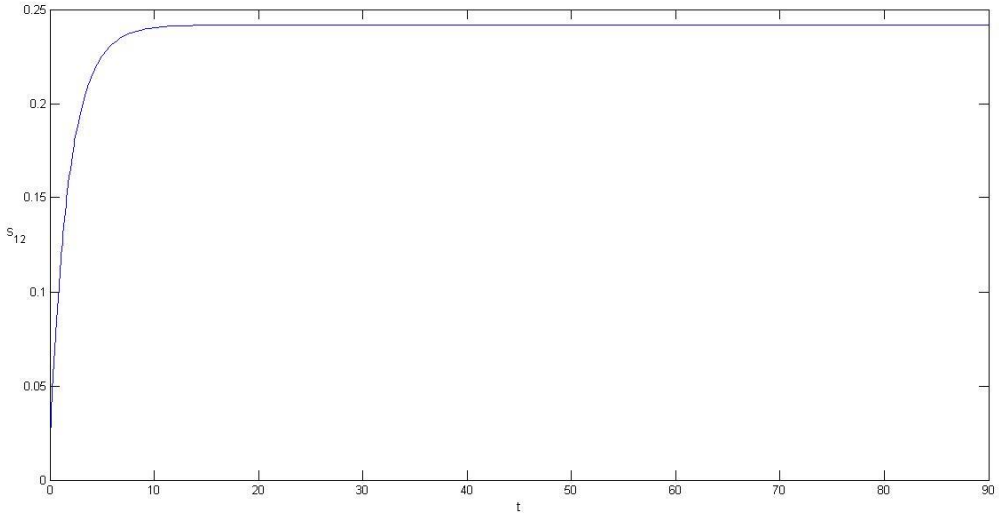

(b)

Figure 4.26: These are simulations recorded at s1f = 50; B2=1.92*10^{-4}; hf=6.17; The other parameters are same as Table 3.4. (a)Profile of $s_{11}(t)$; (b) Profile of $s_{11}(t)$

A high value of ACh feed concentration is taken to investigate the ability of AChE to degrade the high concentration of ACh. The results above depict the efficiency of AChE to degrade ACh concentration from a 25 in (a) to 0.24 in (b). The explanation for this is that there is a competition between diffusion process of transfer of ACh from compartment 1 to 2 and enzymatic process. Because AChE works at a higher efficiency, enzymatic process is much faster than diffusion.

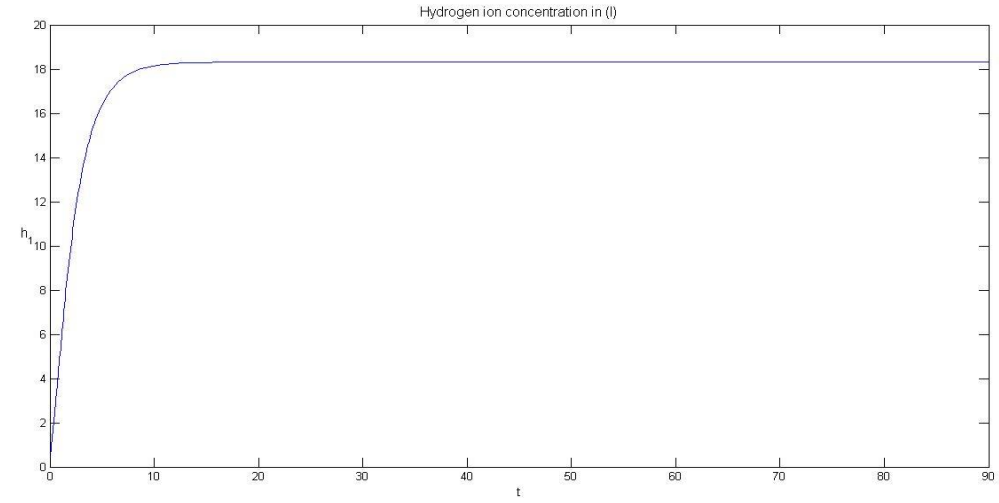

(a)

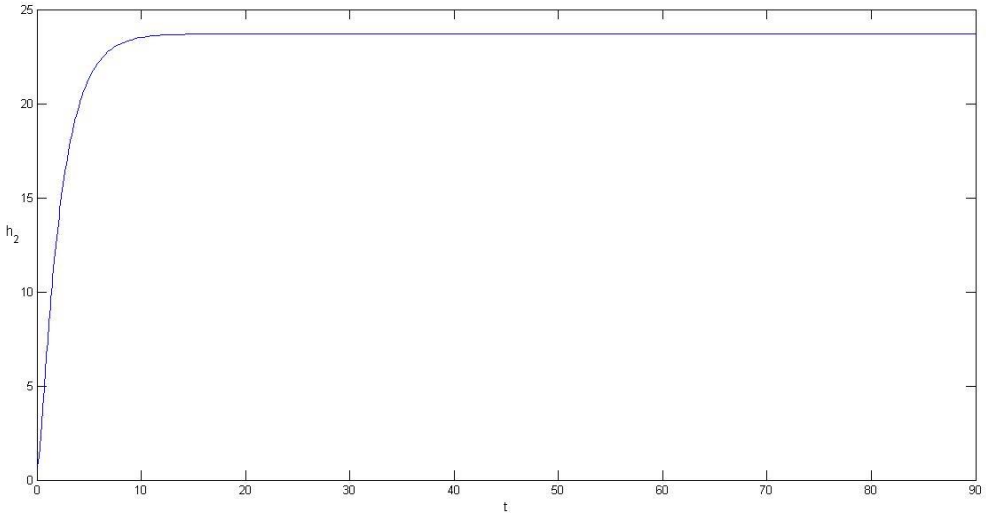

(b)

Figure 4.27: s1f=50; hf=6.17; B2=0.5*10^{-4}; (a) Profile of h_1(t); (b) Profile of h_2(t)

The pH rises from 18 in (a) to 23 in (b). According to Elnashaie, S.S.E.H.; El-Rifai, M.A.; Ibrahim, G. (1983) , $B_2 < 0.899*10^{-4}$ is a multiplicity region. The presence of this region has its effects on the behavior of the system to respond to external disturbances that may move the system into this multiplicity region. This phenomena helps the system to respond to external disturbances like inhibition of AChE by β-amyloid aggregates or treating Alzheimer's disease which is based on inhibiting AChE to increase ACh concentration.

C) FEED ACh CONCENTRATION

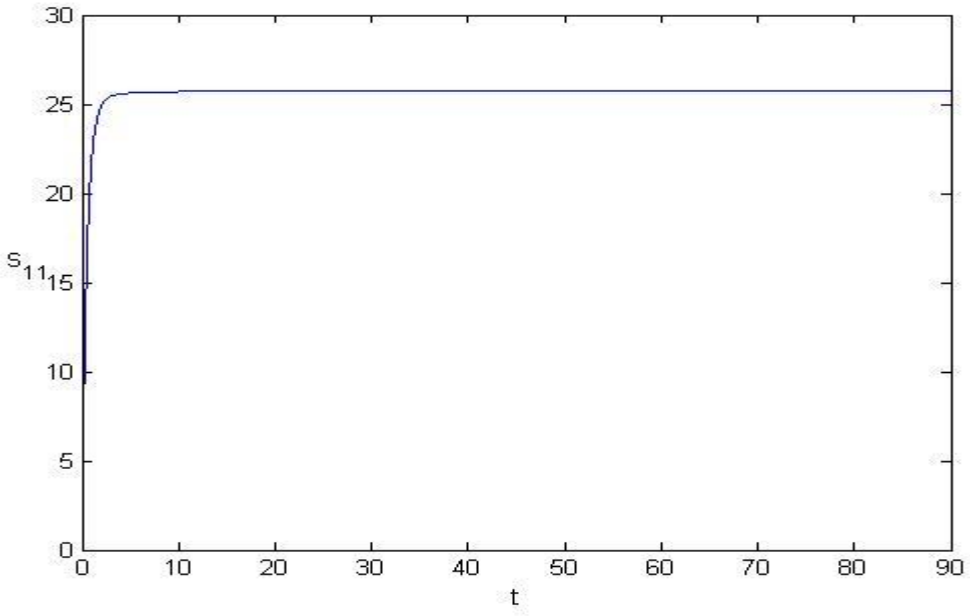

(a)

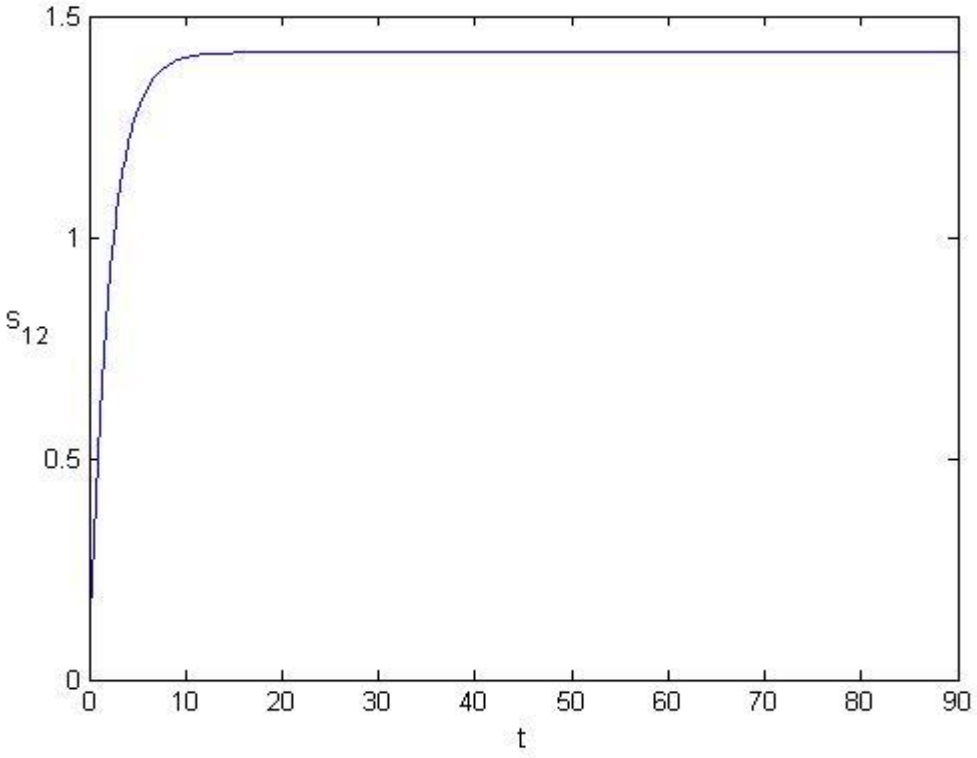

(b)

Figure 4.28: s_{1f} = 50; h_f = 6.17; (a) Profile of s_{11}(t); (b) Profile of s_{12}(t)

The system is characterized by stationary state in Figure 4.28. High concentration of s_{1f} exists. Rate of enzyme activity < Rate of diffusion. Hydrolysis reaction in 2 may be inhibited by excess ACh.

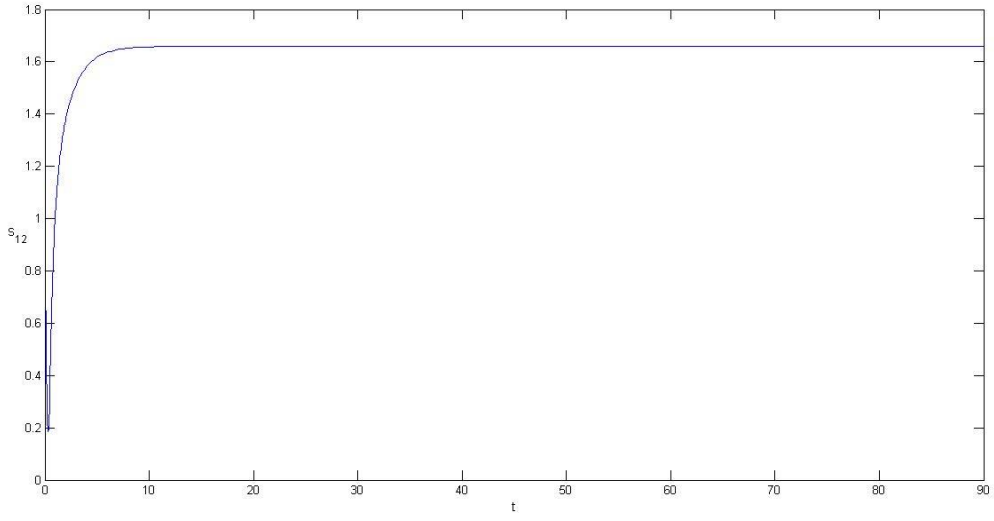

(a)

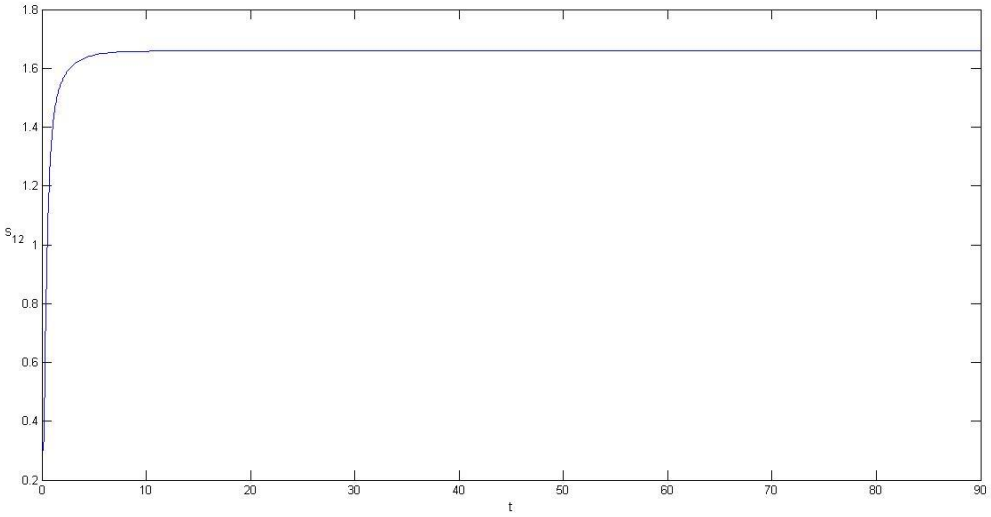

(b)

Figure 4.29: s_{1f} = 2.398; h_f = 0.002; B_1=0.0001; B_2 = 0.0002; s_{2f} = 3; s_{3f} = 2; (a) Profile s_{12}(t) at initial values [0.004,3.6,3.23,8.1,0.0498,0.8,1.159,4.9]; s_{12}(t) at initial values [0.003796824,3.8971322,3.233,8.2517318,0.14058,0.280188,1.1606,4.9606]; here initial values are given as [h_1,s_{11}, s_{21}, s_{31}, h_2, s_{12}, s_{22}, s_{32}]

The same value of s_{1f} can lead to different types of solution for different initial conditions. ACh concentration in (a) falls from0.63 to 0.2 and then rises up again to a steady value. In (b) ACh concentration simply rises from 0.3 to reach steady state.

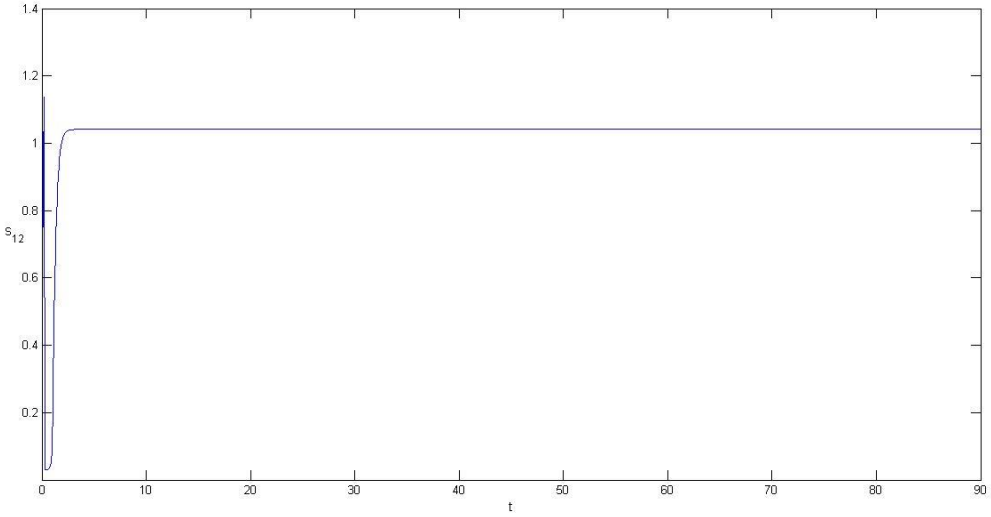

(a)

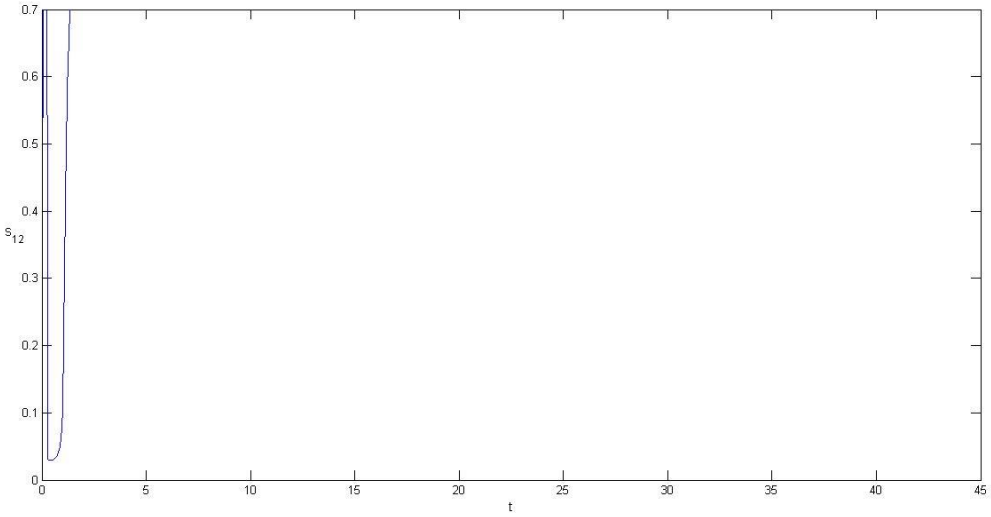

(b)

Figure 4.30: s_{1f} = 3.95135; h_f = 0.002; B_1=0.0001; B_2 = 0.0002; s_{2f} = 3; s_{3f} = 2; (a) Profile of $s_{12}(t)$ (b) Magnified image of the lower profile of $s_{12}(t)$

Figure 4.30 focuses on the graphical behavior mentioned in figure 4.29 (a). The system oscillates for about 1 time unit and then reaches steady state. The graph starts at ACh concentration 0.55.

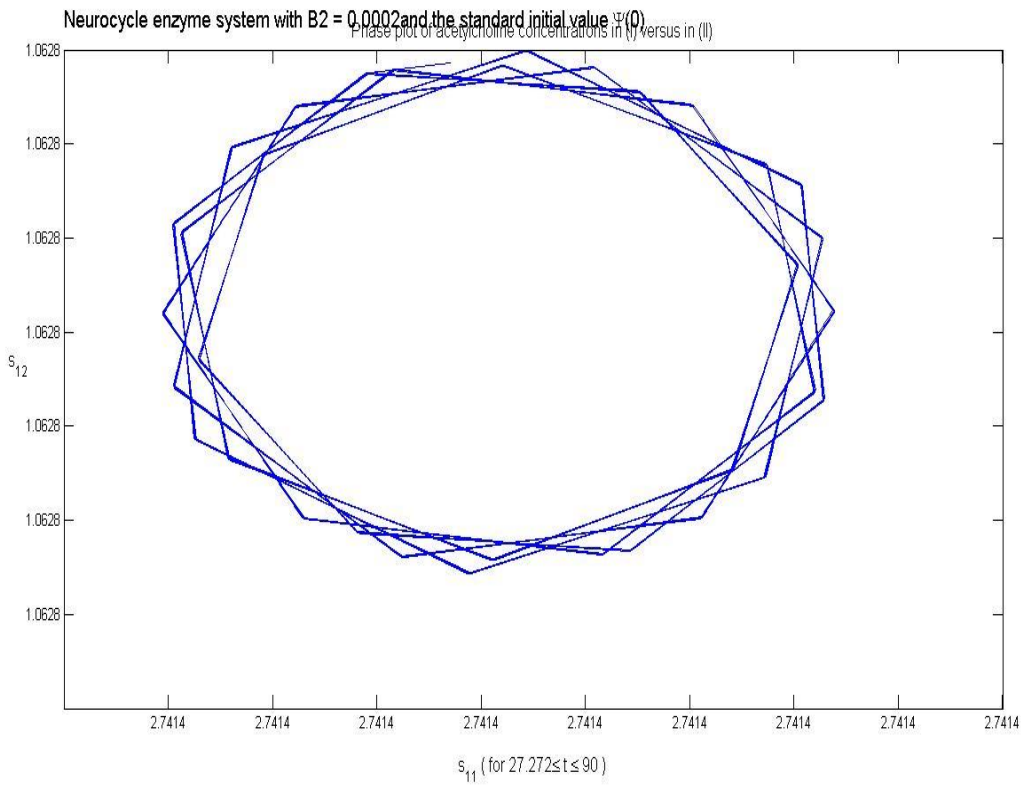
Neurocycle enzyme system with B2 = 0.0002and the standard initial value Ψ(0)
Phase plot of acetylcholine concentrations in (I) versus in (II)
1.0628
1.0628
1.0628
1.0628
1.0628
1.0628
1.0628
s_{12}
2.7414
2.7414
2.7414
2.7414
2.7414
2.7414
2.7414
2.7414
s_{11} (for 27.272≤t≤90)

(a)

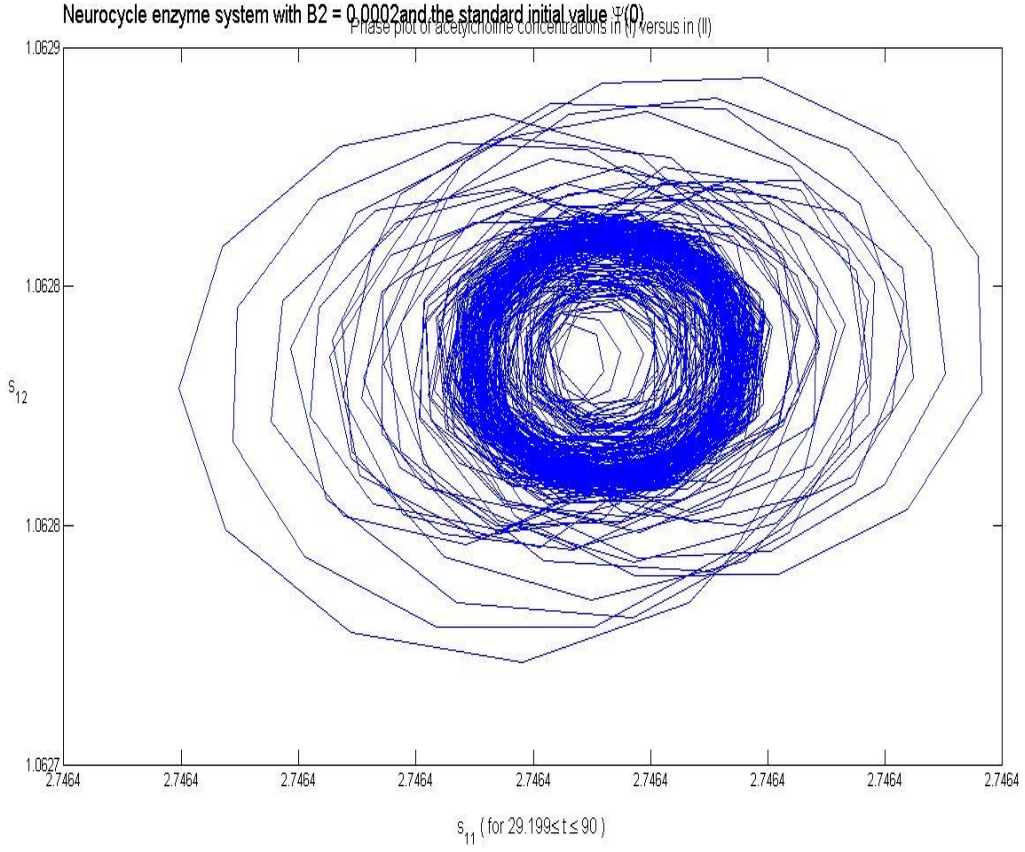
Neurocycle enzyme system with B2 = 0.0002and the standard initial value Ψ(0)
Phase plot of acetylcholine concentrations in (I) versus in (II)
1.0629
1.0628
1.0628
1.0627
s_{12}
2.7464
2.7464
2.7464
2.7464
2.7464
2.7464
2.7464
2.7464
s_{11} (for 29.199≤t≤90)

(b)

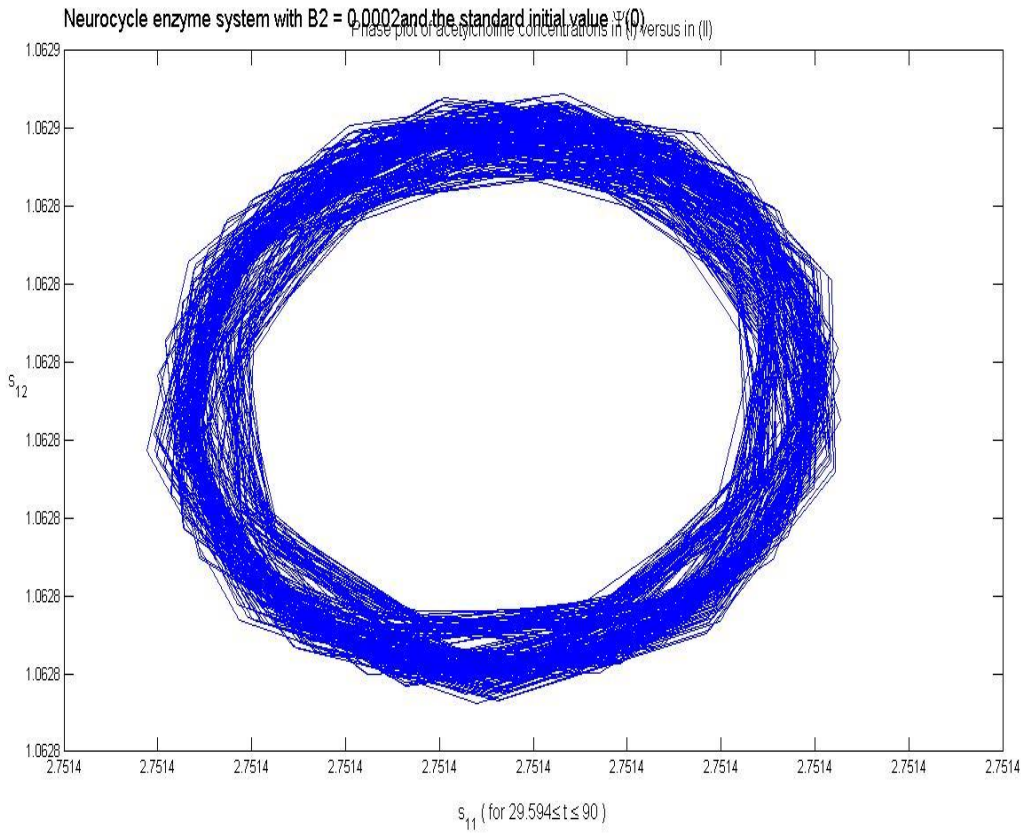
Neurocycle enzyme system with B2 = 0.0002and the standard initial value Ψ(0)
Phase plot of acetylcholine concentrations in (I) versus in (II)
1.0629
1.0629
1.0628
1.0628
1.0628
1.0628
1.0628
1.0628
1.0628
1.0628
S12
2.7514
2.7514
2.7514
2.7514
2.7514
2.7514
2.7514
2.7514
2.7514
2.7514
S11 (for 29.594≤t≤90)

(c)

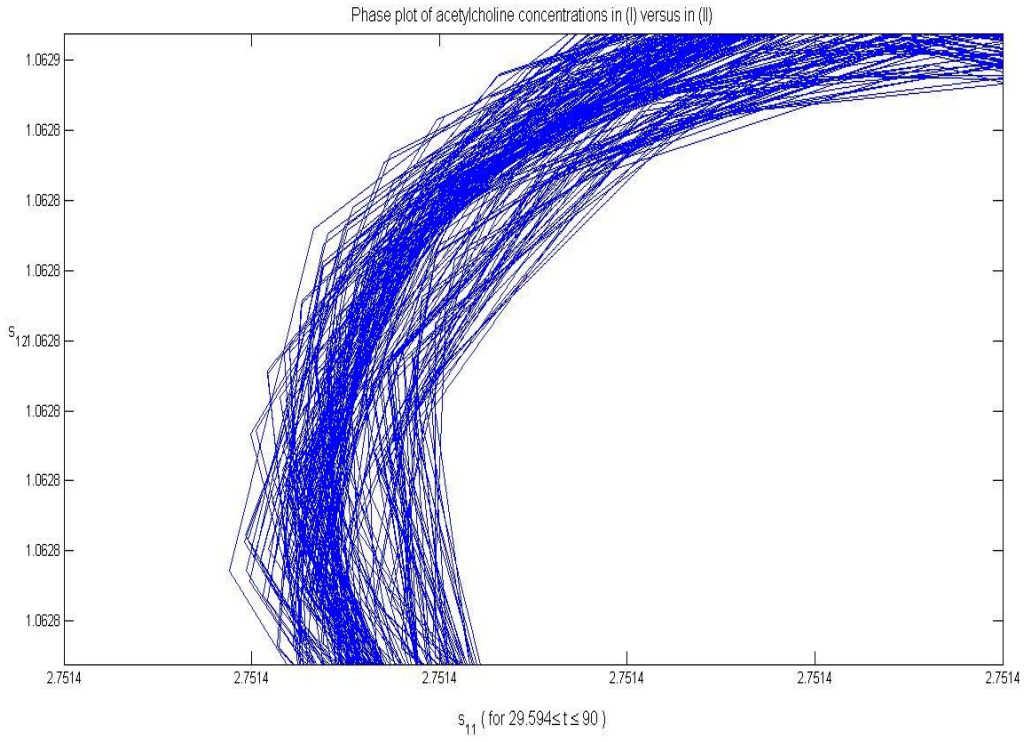
Phase plot of acetylcholine concentrations in (I) versus in (II)
1.0629
1.0628
1.0628
1.0628
1.0628
1.0628
1.0628
1.0628
1.0628
S12
2.7514
2.7514
2.7514
2.7514
2.7514
2.7514
S11 (for 29.594≤t≤90)

(d)

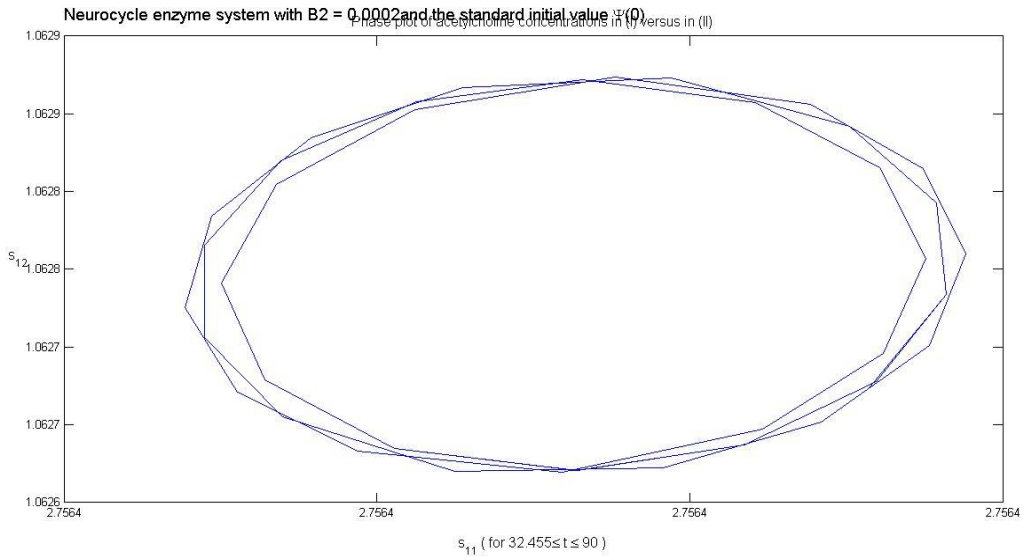

(e)

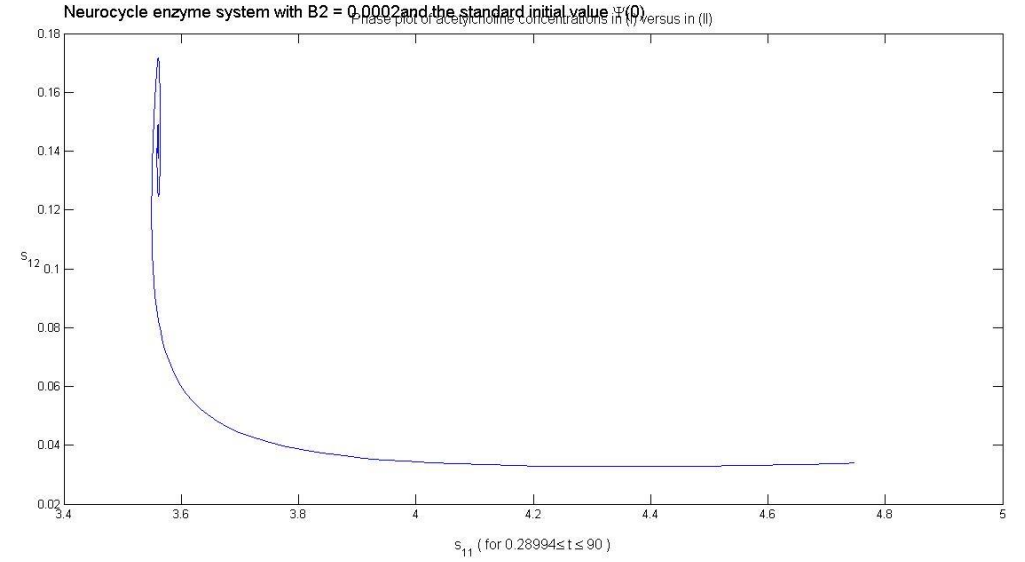

(f)

Figure 4.31: h_f = 0.002; B_1=0.0001; B_2 = 0.0002; s_{2f} = 3; s_{3f} = 2; Phase profiles of s_{12} at s_{1f} equals (a) 4.42; (b) 4.43;(c) 4.44; (d) Magnified version of 4.44; (e) 4.45; (f) 6.98

Figure 4.31 (a) marks the onset of unstable periodic orbits. With increasing s_{1f} these periodic orbits decrease with small amplitudes. These orbits represent an element of order within chaos.

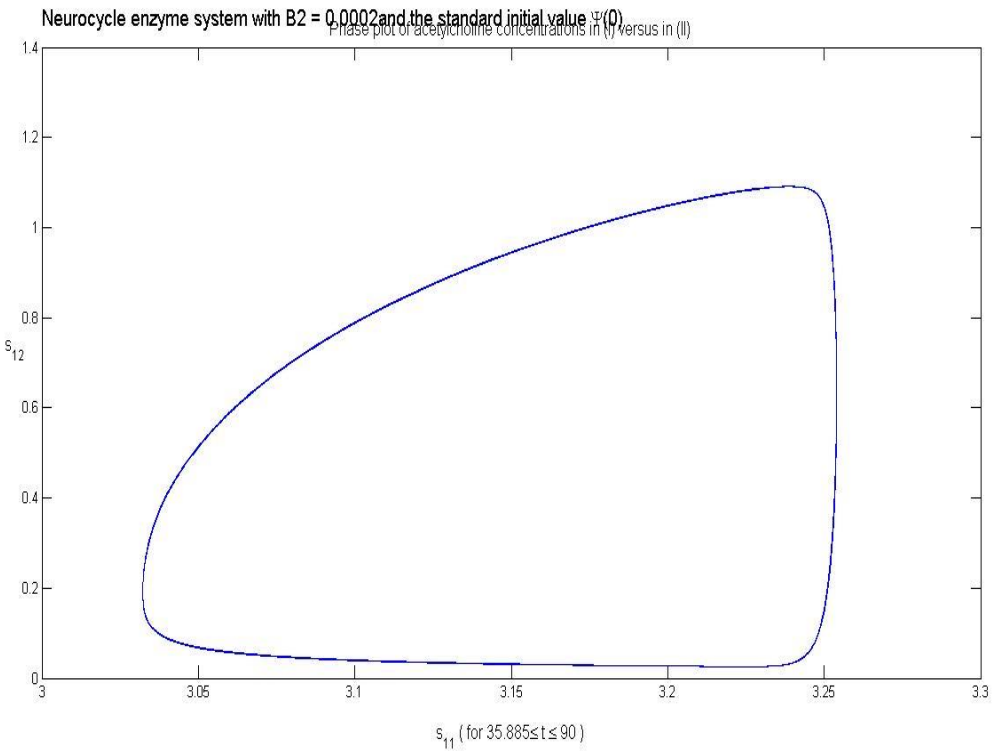
Neurocycle enzyme system with B2 = 0.0002and the standard initial value Ψ(0)
Phase plot of acetylcholine concentrations in (I) versus in (II)
1.4
1.2
1
0.8
0.6
0.4
0.2
0
s12
3
3.05
3.1
3.15
3.2
3.25
3.3
s11 (for 35.885≤ t ≤ 90)

(a)

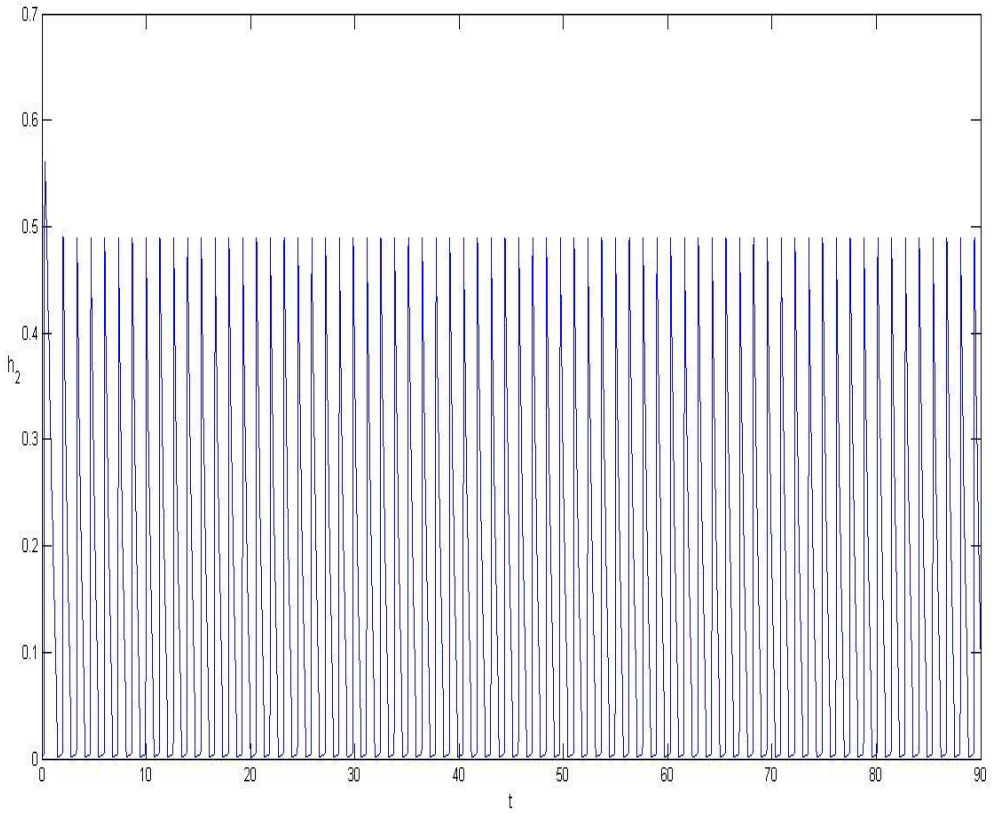
0.7
0.6
0.5
0.4
0.3
0.2
0.1
0
h2
0
10
20
30
40
50
60
70
80
90
t

(b)

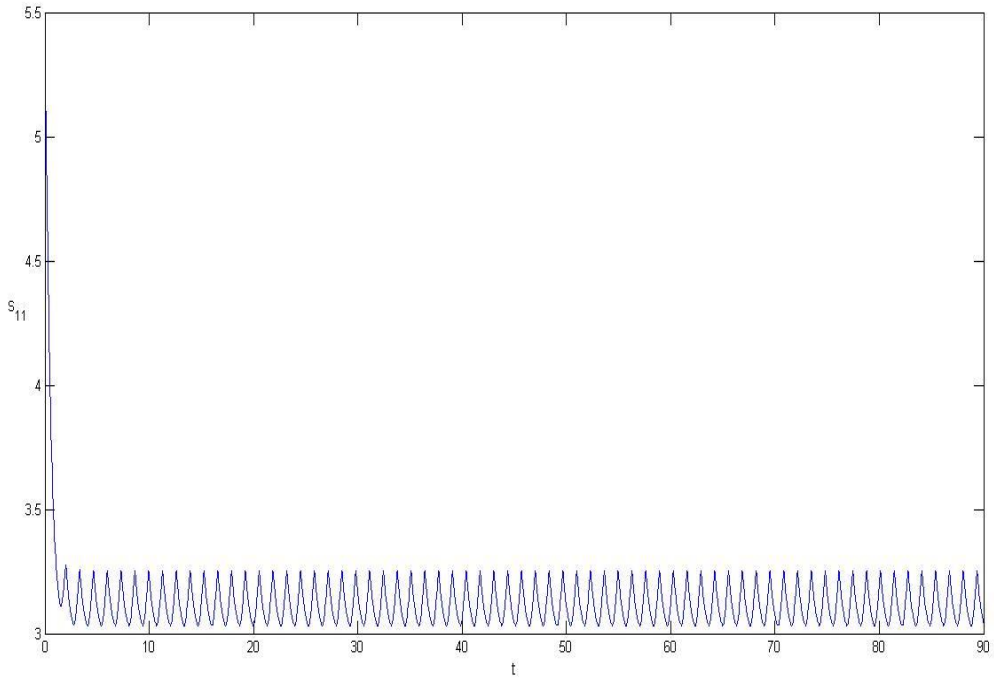
5.5
5
4.5
S_{11}
4
3.5
3
0
10
20
30
40
50
60
70
80
90
t

(c)

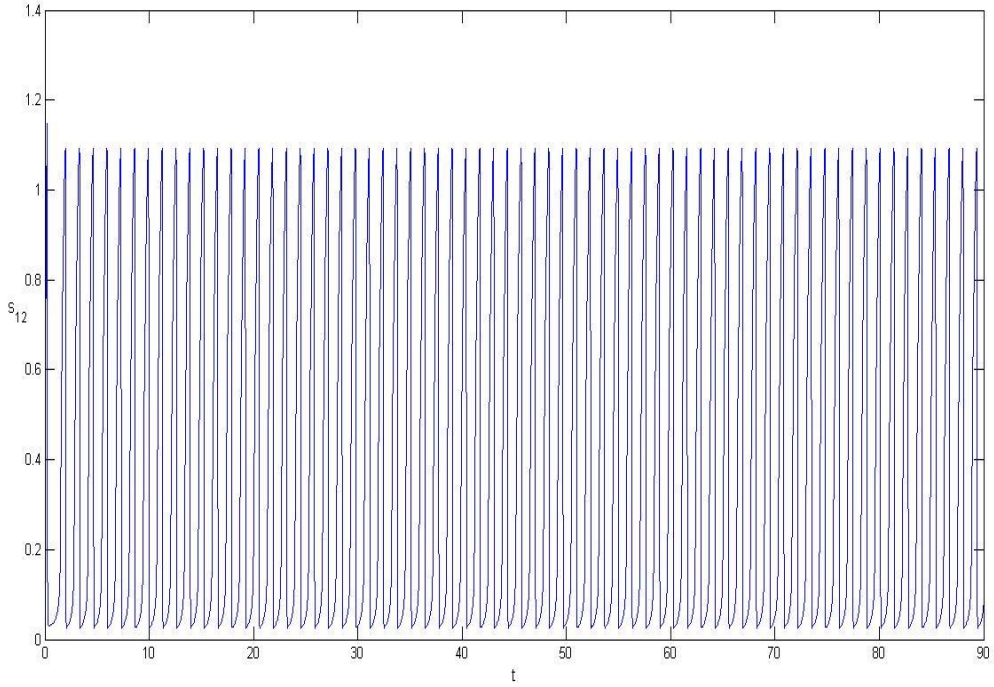
1.4
1.2
1
0.8
S_{12}
0.6
0.4
0.2
0
0
10
20
30
40
50
60
70
80
90
t

(d)

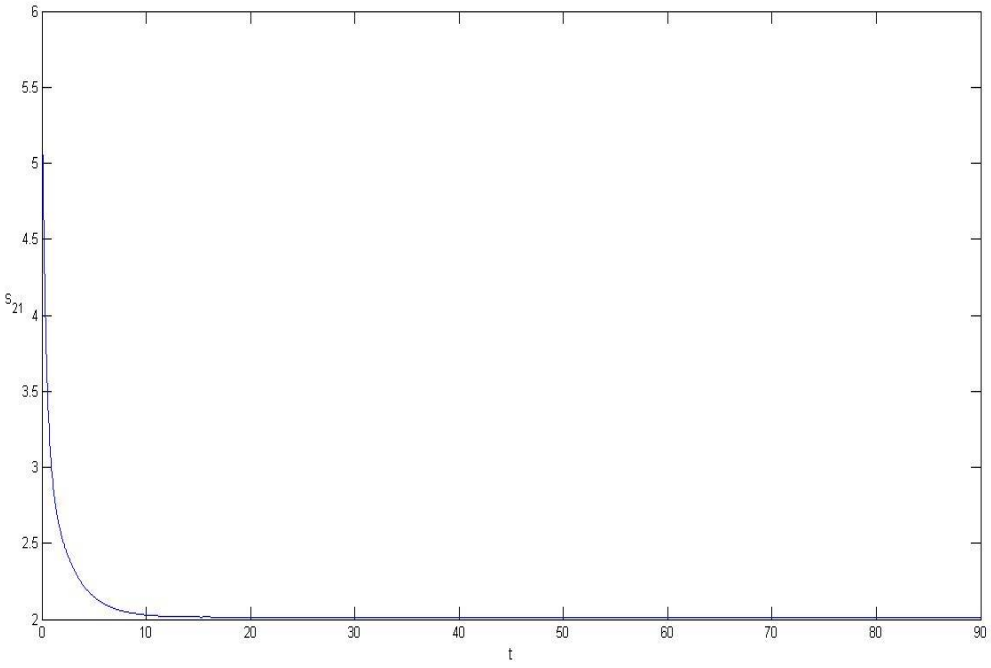
6
5.5
5
4.5
4
3.5
3
2.5
2
S_{21}
0
10
20
30
40
50
60
70
80
90
t

(e)

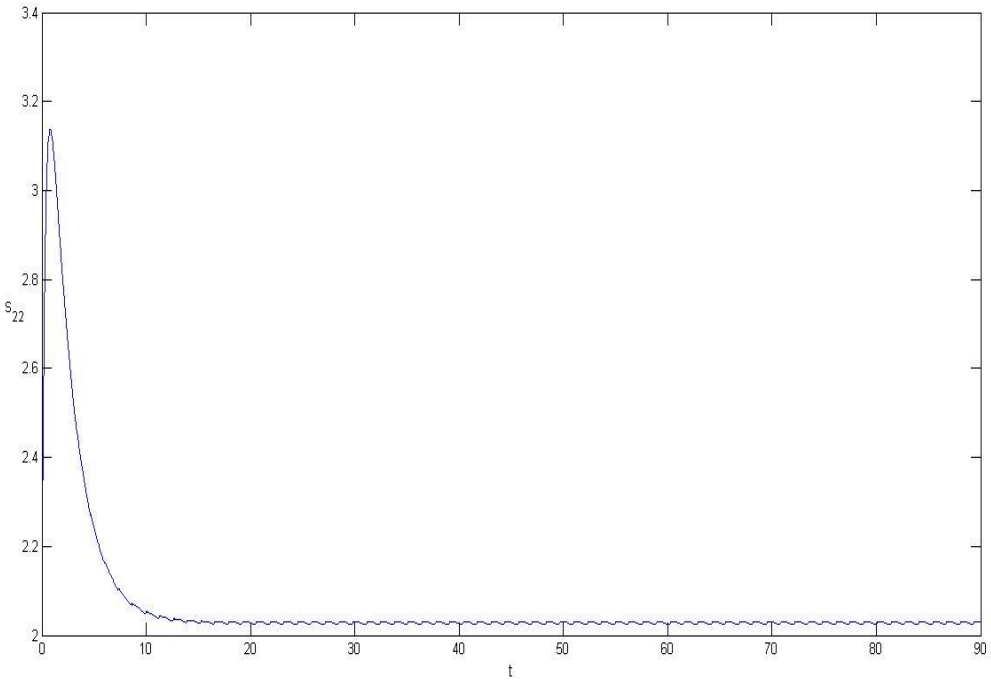
3.4
3.2
3
2.8
2.6
2.4
2.2
2
S_{22}
0
10
20
30
40
50
60
70
80
90
t

(f)

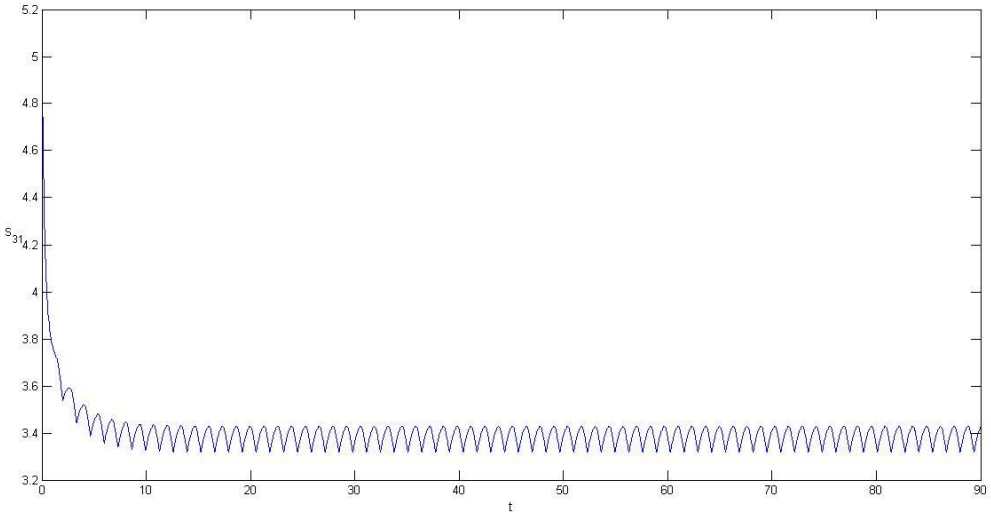

(g)

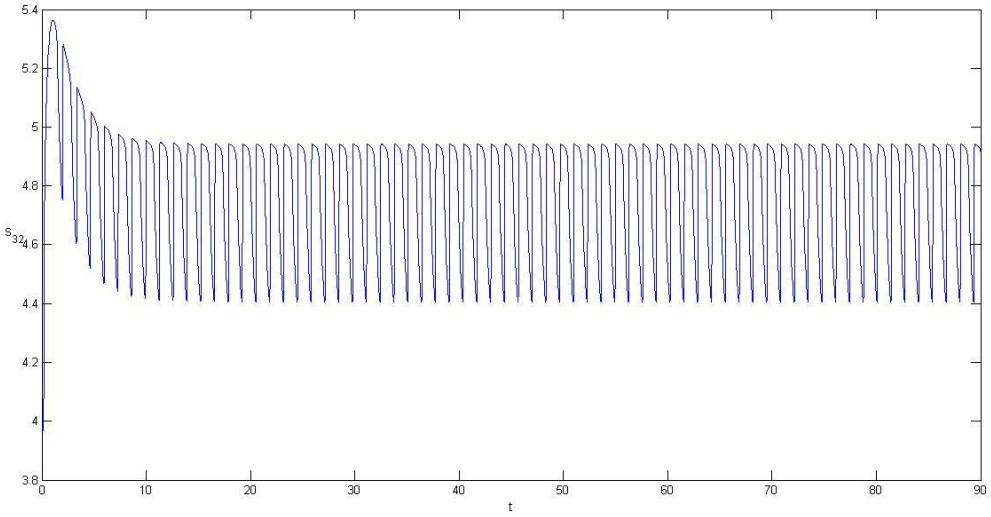

(h)

Figure 4.32: h_f = 0.002; B_1=0.0001; B_2 = 0.0002; s_{2f} = 3; s_{3f} = 2; At s_{1f} = 5.87254 profiles of (a) Phase profile; (b) $h_2(t)$; (c) $s_{11}(t)$; (d) $s_{12}(t)$; (e) $s_{12}(t)$; (f) $s_{22}(t)$; $s_{31}(t)$; $s_{32}(t)$

The above graphs depict the chaotic behavior at s_{1f} = 5.87254. All parameters vary as one period limit cycle and cause disturbances in the neural enzyme system leading to multiples defects like memory loss, lack of motor skills etc. ACh feed cocncentration in the range 4.44 to 6.98 is not healthy for brain activity.

(D) β-AMYLOID AGGREGATES

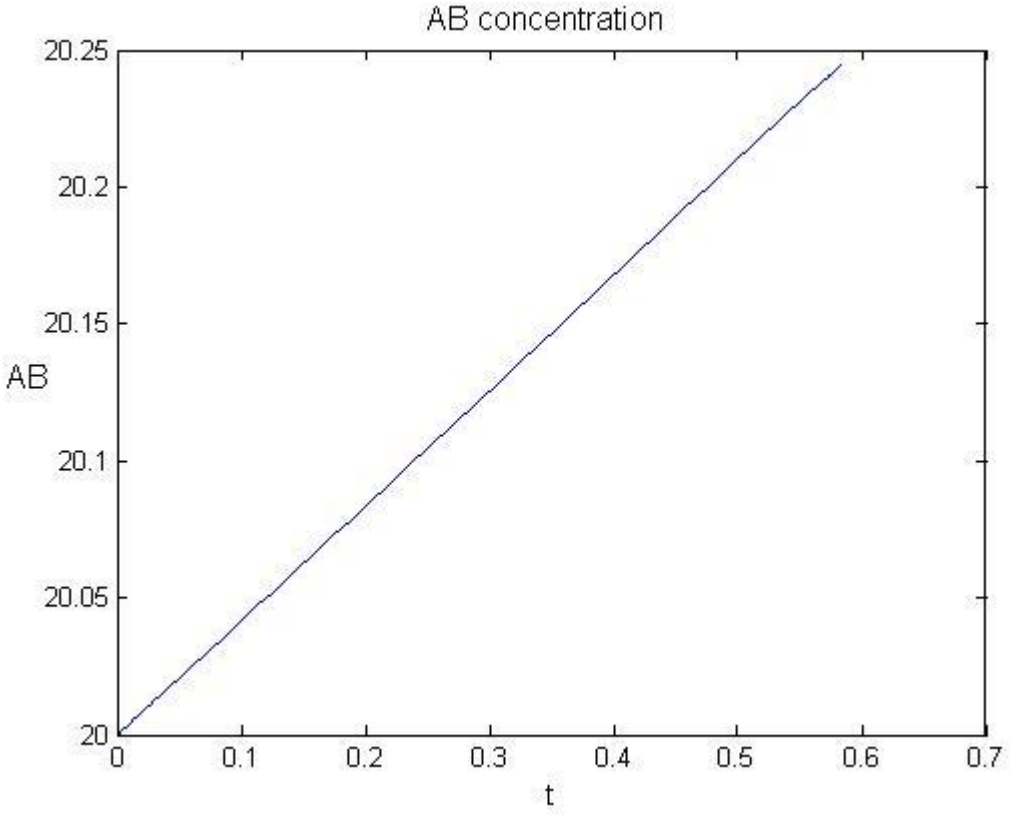

(a)

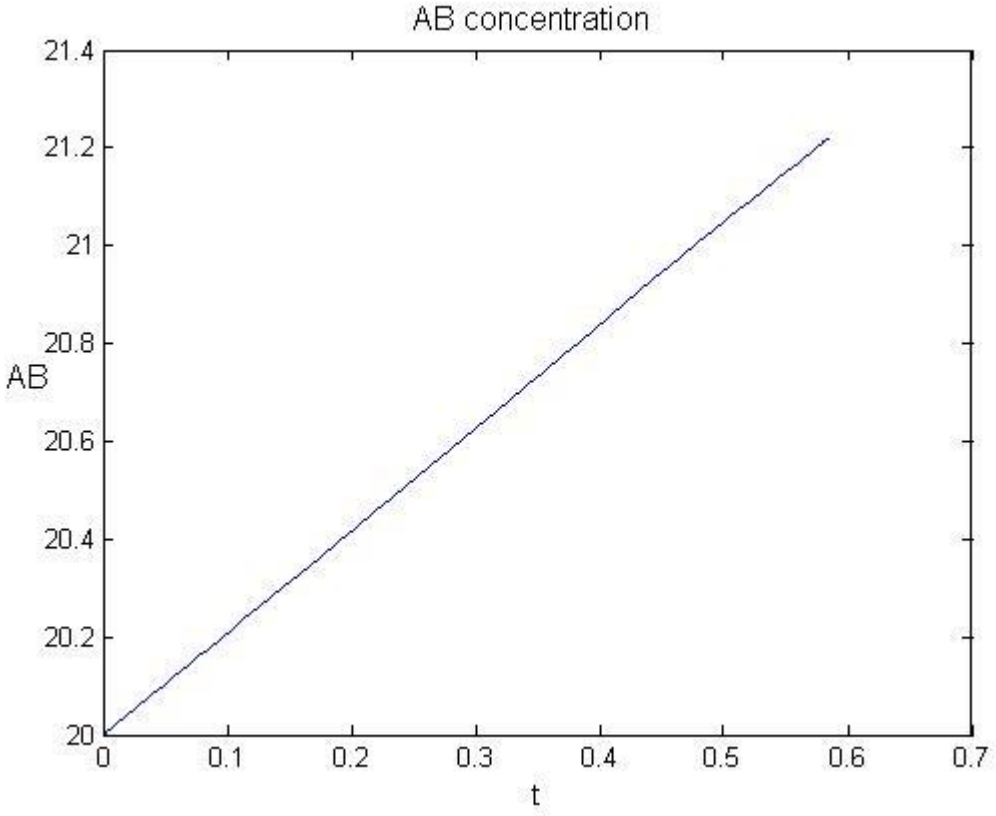

(b)

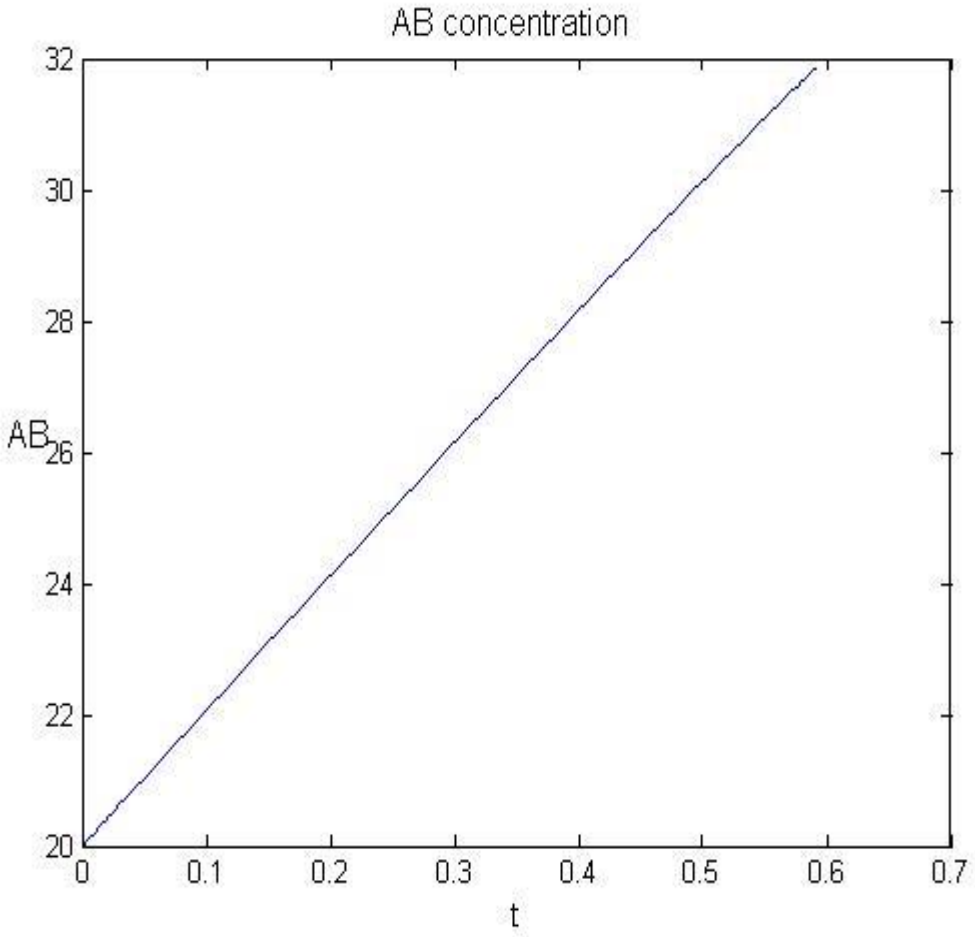

(c)

Figure 4.33: The variation of β-amyloid aggregate concentration for KL_2 equals (a) 0.5; (b) 2.5; (c) 25

We can clearly see that for the same time interval (c) has maximum concentration followed by (b) and then (a). Hence we can conclude that when KL_2 increases, the concentration of β-amyloid aggregate increase.

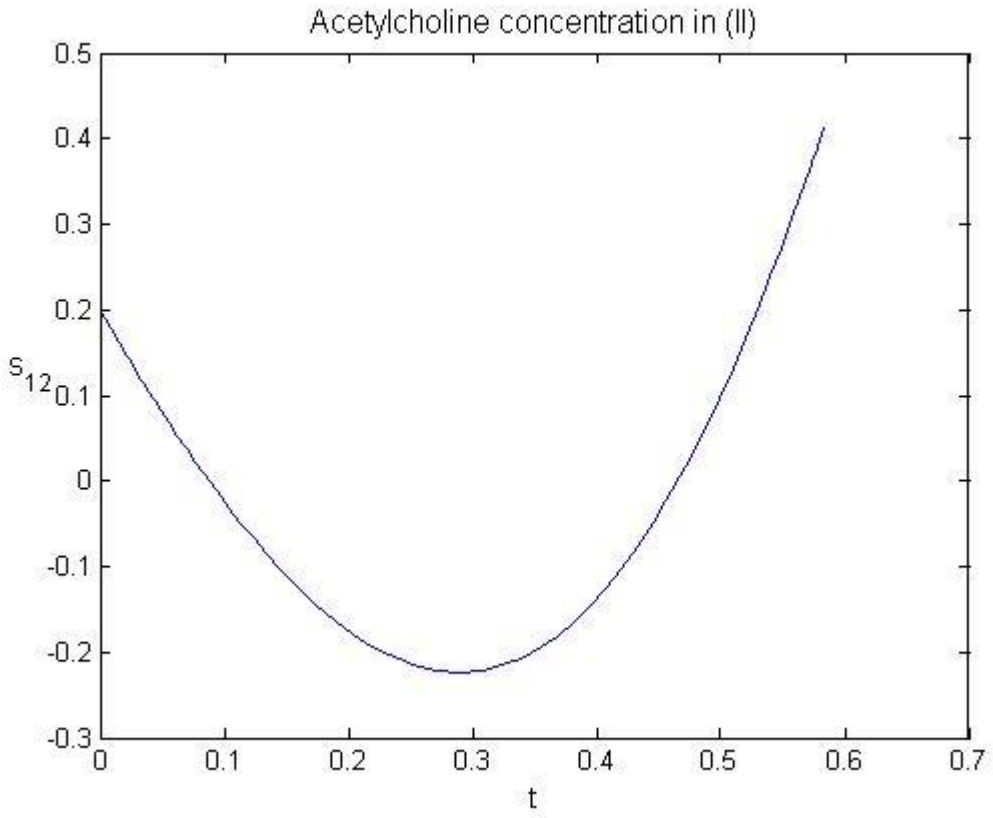

Figure 4.34: Profile of $s_{12}(t)$ with KL_2 equals 0,0.5,2.5 and 25

ACh concentration in compartment 2 (s_{12}) does not change with KL_2. s_{12} level is mainly governed by 2 processes, membrane diffusion and rate of ACh degradation. The transport of ACh into compartment 2 through membrane diffusion decreases slightly due to reduced s_{11} levels from β-amyloid inhibition. The rate of ACh breakdown is maintained the same. The influx of ACh into compartment 2 is approximately an order of magnitude higher than the consumption of ACh in that compartment. Therefore although the influx of ACh into compartment 2 is limited by β-amyloid inhibition, r_2 is so small that the level of s_{12} is not affected.

5. CONCLUSIONS

1) An eight-dimensional model has been developed, solved, and analyzed for a coupled acetylcholinesterase/choline acetyltransferase enzyme system. The complex dynamic characteristics, both stable and unstable, and the chaotic behavior of this IVP system have been investigated with some reference to acetylcholine neural transmission. The variation of the hydrogen-ion feed concentration h_f as bifurcation parameter has a strong effect on the state variables at low concentrations, in contrast to its weak effect at high concentrations. At low concentrations it is found that a complex dynamic behavior with period doubling, period adding, and period subtracting dominate the dynamics of the system. Checking for a possible correspondence to physiological values for the pH values, we can say that compartment (II) (where the pH level is between 6.73 and 7.97 for the studied variations of h_f) has a pH value near to the expected value for the human brain. This represents a complex biological example that sheds some light on the relation between enzyme activities in the brain and Alzheimer's and Parkinson's diseases.
2) The results of varying B_2 implies that AChE enzyme activity exhibits oscillatory behavior at the low concentrations. It is found that the system is not influenced clearly at low pH_f. The results are in accordance with the physiological and experimental and theoretical reviews. From investigating AChE enzyme as the bifurcation parameter, an oscillatory behavior of ACh is witnessed for a certain specific range of B_2. This range of B_2 ultimately gives rise to certain abnormalities in the production and release of ACh neurotransmitter. Any malfunction in this neurocycle enzyme system can lead to cholinergic disorders. The enzyme system has a capability to respond to any forcing disturbances affecting the cholinergic ACh system to be able to regulate its components to adapt to any sudden changes. The feedback mechanism of the system can work as a vital control device to control and regulate the transmission activity and the processes of the ACh in both compartments. The findings of this research can be useful to be able to understand the characteristics and the behavior of the ACh cholinergic system and discover the disturbances in the enzymatic processes occurring in the system. In addition, the relation between the neurological sicknesses like Alzheimer's and Parkinson's disease and the complex dynamics and chaotic behavior of the ACh system can be helpful for enriching more research on other disorders in living organisms.

3) The results obtained from studying the effect of bifurcation parameters such as (the feed hydrogen ions concentrations and the AChE enzyme activity and feed ACh concentrations) assures the presence of oscillatory behavior at the low concentrations of these parameters. It is found that the system is not influenced clearly at low h_f. The results are in accordance with the physiological and experimental and theoretical reviews. One of the main explanations is that the high concentrations of H^+ will inhibit choline diffusion into presynaptic membrane, another explanation is that the high concentrations may inhibit the synthesis and hydrolysis reaction and finally will cause the state variables to approach the plateau. The choline recycled from the postsynaptic neurons to be reused in the presynaptic neurons is taken into consideration and will help the system to control and regulate the levels of the state variables in both compartments.
4) The effect of β-amyloid peptide as an inhibitor on ChAT activity for ACh synthesis through the two enzyme/two compartment (2E2C) model in a variety of situations is analyzed. Overall, numerical solutions to the modified 2E2C with β-amyloid were in accordance with three significant, widely reported symptoms of AD; loss of ChAT activity and reduced ACh production (Pederson 1996). This in turn means that the direct inactivation of ChAT by β-amyloid may be a probable mechanism contributing to the development of AD. The incorporation of ChAT inhibition by β-amyloid into the 2E2C model is able to yield dynamic solutions for concentrations of generated β-amyloid and ACh hydrolysis in compartment 1 and 2. This correlates well to the physiological understanding since the production of β-amyloid is not generally known to be highly reversible. One of the most significant physiological symptoms of AD is the reduction of ACh neurotransmitter concentration within cholinergic neurons. In this investigation, the effect of ChAT activity inhibition via β-amyloid is considered an individual basis in order to evaluate the validity of kinetic mechanism.

6. REFERENCES

1) Jean-Pierre Bellier and Hiroshi Kimura (2007), Acetylcholine synthesis by choline acetyltransferase of a peripheral type as demonstrated in adult rat dorsal root ganglion, Journal of Neurochemistry Volume 101 Issue 6 1607-1618.
2) Mustafaa I H, G. Ibrahim, A. Elkamel, S.S.E.H. Elnashaie, P. Chen, (2009), Non Linear Feedback Modeling and Bifurcation of the Acetylcholine Neurocycle and its Relation to Alzheimer's and Parkinson's Diseases; accepted by Journal of chemical engineering science 64(1), 69-90.
3) Elnashaie, S.S.E.H.; El-Rifai, M.A.; Ibrahim, G. (1983) The effect of hydrogen ion production on the steady-state multiplicity of substrate inhibited enzymatic reactions steady-state considerations. Applied Biochemistry and Biotechnology, 8, 275.
4) Elnashaie, S.S.E.H.; El-Rifai, M.A.; Ibrahim, G. (1983). The effect of hydrogen ion production on the steady-state multiplicity of substrate inhibited enzymatic reactions. II: Transient behavior. Applied Biochemistry and Biotechnology, 8, 467.
5) Elnashaie, S.S.E.H.; El-Rifai, M.A.; Ibrahim, G. (1984) The effect of hydrogen ion production on the steady-state multiplicity of substrate inhibited enzymatic reactions. III: asymmetrical steady-states in enzyme membranes. Applied Biochemistry and Biotechnology, 9, 455.
6) Elnashaie, S.S.E.H.; Ibrahim, G.; Teymour, F. A (1995). Chaotic behavior of an acetyl cholinesterase enzyme system. Chaos, Solitons & Fractals. 5, 933.
7) Garhyan P., Mahecha A Botero ; Elnashaie, S.S.E.H.; (2006). Complex Bifurcation/ Chaotic Behavior of Acetylcholinesterase and Cholineacetyltransferase Enzymes system; Mathematical and Computer Modeling; 30 824-853
8) Tucek, S., (1978). Acetylcholine Synthesis in Neurons; Champan & Hall, London. 1978.
9) Tucek, S. (1985). Regulation of acetylcholine synthesis in the brain. Journal of Neurochemistry, 44:11-24.
10) Elnashaie S. S.E., Uhlig F., and Affane C.b , 2005, Numerical techniques for chemical and biological engineers using MATLAB : a simple bifurcation approach, New York : Springer, 2007.
11) Garhyan Parag, Mahecha A Botero; Elnashaie, S.S.E.H.; (2006). Complex Bifurcation/ Chaotic Behavior of Acetyl cholinesterase and choline Acetyltransferase Enzymes system; Mathematical and computer Modeling; 30 824-853

12) Ibrahim, G; Elnashaie, S.S.E.H. Hyperchaos in acetyl cholinesterase enzyme systems. Chaos, Solitons & Fractals.(1997), 8, 1977.
13) Mahecha Andres - Botero, Parag Garhyan, Elnashaie S. S. E. H., (2004). Bifurcation and chaotic of a coupled acetylcholinesterase/choline acetyltransferase diffusion-reaction enzymes system, Chemical Engineering Science 59,581-597.
14) Mustafaa I H, G. Ibrahim, A. Elkamel, S.S.E.H. Elnashaie, P. Chen, (2009), Effect of Choline and Acetate Substrates on Bifurcation and Chaotic Behavior of Acetylcholine Neurocycle and Alzheimer's and Parkinson's Diseases; Journal of chemical engineering science. 64(9), 2096-2112.
15) Mustafa I. , A. Elkamel, A. Lohi P. Chen, S.S.E.H. Elnashaie, G. Ibrahim, (2012), Application of Continuation Method and Bifurcation for Acetylcholine Neurocycle Considering Partial Dissociation of Acetic Acid, Computers an Chemical Engineering 46 (2012) 78-93
16) Mustafa I H, G. Ibrahim, A. Elkamel, S.S.E.H. Elnashaie, P. Chen, (2012), Effect of Cholineacetyltransferase Activity and Choline Recycle Ratio on Modelling, Bifurcation and Chaotic Behavior of Acetylcholine Neurocycle and Their Relation to Alzheimer's and Parkinson's Diseases; Journal of Chemical Engineering Science, 68(1), 19-35
17) Zheng WH, Bastianetto S, Mennicken F, Ma W, Kar S, Amyloid β-peptide induces tau phosphorylation and neuronal degeneration in rat primary septal cultured neurons. Neuroscience 2002;115:201-11.
18) Asmaa Abdallah Awad, (2013) Pharmacokinetics/Pharmacodynamics and Analysis of the Effect of β-Amyloid Peptide on Acetylcholine Neurocycle and Alzheimer's Disease Medications, 2013